

**Lepton flavor violation and  $\theta_{13}$  in minimal resonant leptogenesis**

Frank F. Deppisch\* and Apostolos Pilaftsis†

*School of Physics and Astronomy, University of Manchester, Manchester M13 9PL, United Kingdom*

(Received 17 December 2010; published 12 April 2011)

We study the impact of minimal nonsupersymmetric models of resonant leptogenesis on charged-lepton flavor violation and the neutrino-mixing angle  $\theta_{13}$ . Possible low-scale flavor realizations of resonant  $\tau$ -,  $\mu$ - and  $e$ -leptogenesis provide very distinct and predictive frameworks to explain the observed baryon asymmetry in the Universe by sphaleron conversion of an individual  $\tau$ -,  $\mu$ - and  $e$ -lepton-number asymmetry which gets resonantly enhanced via out-of-equilibrium decays of nearly degenerate heavy Majorana neutrinos. Based on approximate flavor symmetries, we construct viable scenarios of resonant  $\tau$ -,  $\mu$ - and  $e$ -leptogenesis compatible with universal right-handed neutrino masses at the grand unified theory scale, where the required heavy-neutrino mass splittings are generated radiatively. The heavy Majorana neutrinos in such scenarios can be as light as 100 GeV and their couplings to two of the charged leptons may be large. In particular, we explicitly demonstrate the compelling role that the three heavy Majorana neutrinos play, in order to obtain successful leptogenesis and experimentally testable rates for lepton-flavor violating processes, such as  $\mu \rightarrow e\gamma$  and  $\mu \rightarrow e$  conversion in nuclei.

DOI: 10.1103/PhysRevD.83.076007

PACS numbers: 11.30.Er, 14.60.St, 98.80.Cq

**I. INTRODUCTION**

The observed baryon asymmetry in the Universe (BAU), which amounts to a baryon-to-photon ratio of number densities  $\eta_B \approx 6.2 \times 10^{-10}$  [1,2], provides one of the strongest pieces of evidence for physics beyond the standard model (SM) [3]. One interesting scenario for explaining the BAU is leptogenesis [4]. Leptogenesis does have a profound link to neutrinos and the origin of their extraordinary small masses. In particular, the famous seesaw mechanism [5] can give rise to their small observed masses through the presence of superheavy Majorana neutrinos close to the grand unified theory (GUT) scale,  $M_{\text{GUT}} \approx 2 \times 10^{16}$  GeV. These GUT-scale heavy neutrinos, being singlets under the SM gauge group, may possess large Majorana masses that violate lepton number ( $L$ ) by two units. In an expanding Friedmann–Lemaître–Robertson–Walker Universe, the heavy Majorana neutrinos can decay out of equilibrium and produce a net leptonic asymmetry. The so-produced leptonic asymmetry gets rapidly reprocessed into the observed BAU [4] by equilibrated  $(B + L)$ -violating sphaleron interactions [6].

A potentially interesting alternative to GUT-scale leptogenesis is the framework of low-scale resonant leptogenesis (RL) [7,8]. Within this framework, the lowering of the scale may rely on a dynamical mechanism, in which heavy-neutrino self-energy effects [9] on the leptonic asymmetry become dominant [10] and get resonantly enhanced [7], when a pair of heavy Majorana neutrinos has a mass difference comparable to the heavy-neutrino decay widths. As a consequence of thermal RL, the heavy Majorana-mass scale can be as low as  $\sim 100$  GeV, while

maintaining agreement with the solar and atmospheric neutrino data [8]. One of the advantages of low-scale RL is that the reheating temperature  $T_{\text{reh}}$  resulting from inflaton decays does not need to be very high, e.g.  $T_{\text{reh}} \sim 1\text{--}10$  TeV [11], thereby avoiding comfortably the overproduction of gravitinos in supersymmetric models whose late decays may cause dissociation of the light elements during the nucleosynthesis era [12].

Flavor effects due to heavy-neutrino Yukawa couplings play an important role in models of RL [13,14]. In particular, in [13], a scenario was put forward, called resonant  $\tau$ -leptogenesis (R $\tau$ L), in which the BAU originates from a  $\tau$ -lepton asymmetry, resonantly produced by quasi-in-equilibrium decays of heavy Majorana neutrinos. This mechanism makes use of the property that sphalerons preserve the individual quantum numbers  $\frac{1}{3}B - L_{e,\mu,\tau}$  [15–18]. In a R $\tau$ L model, the generated excess in the  $L_\tau$  number will be converted into the observed BAU, provided the  $L_\tau$ -violating reactions are not strong enough to wash out such an excess. In such a scenario, the heavy Majorana neutrinos can be as light as 100 GeV and have sizeable couplings to two of the charged leptons, specifically to electrons and muons. Consequently, depending on the flavor dynamics of heavy-neutrino Yukawa-coupling effects, phenomenologically testable models of RL can be built that could be probed at the LHC or in low-energy experiments of lepton-number violation and lepton-flavor violation (LFV). For instance, observables of particular interest are the neutrinoless double-beta ( $0\nu\beta\beta$ ) decay of heavy nuclei [19], the photonic decay  $\mu \rightarrow e\gamma$  analyzed by the MEG experiment [20] and the coherent  $\mu \rightarrow e$  conversion in nuclei to be looked for in the planned COMET/PRISM experiment [21].

In this paper we study all possible alternatives to R $\tau$ L, including the minimal models of resonant  $\mu$ -leptogenesis

\*frank.deppisch@manchester.ac.uk

†apostolos.pilaftsis@manchester.ac.uk

( $R\mu L$ ) and resonant  $e$ -leptogenesis ( $ReL$ ). Collectively, we refer to these three different lepton-flavor realizations of RL as  $R\ell L$ . We assume that the  $R\ell L$  models have an SO(3)-symmetric heavy-neutrino mass spectrum at the GUT scale, with all heavy Majorana neutrinos being exactly degenerate at this scale. We consider a minimal nonsuper-symmetric framework, in which the heavy-neutrino mass splittings required for successful RL are generated radiatively [22] and can therefore be naturally comparable to the decay widths of the heavy neutrinos. Since all charged-lepton Yukawa couplings are in thermal equilibrium at temperatures  $T \lesssim 10$  TeV [23], we consider a flavor diagonal basis for these couplings, while setting up the Boltzmann equations (BEs). In addition, we include the flavor effects due to individual heavy-neutrino Yukawa couplings [13,24], which can have a dramatic impact on the predictions for the BAU in RL models [13,14].

The layout of the paper is as follows. Section II describes the basic structure of the minimal SM with three heavy Majorana neutrinos and introduces the flavor symmetries needed to realize the different lepton-flavor scenarios associated with  $R\ell L$ . As mentioned above, we assume a SO(3) symmetric heavy-neutrino sector at the GUT scale and calculate the renormalization-group (RG) effects on the mass spectrum of the electroweak-scale heavy Majorana neutrinos and their Yukawa couplings to charged leptons. Taking the light-neutrino oscillation data into account, we are able to determine most of the theoretical parameters of the  $R\ell L$  models. In Sec. III, we present analytic results and predictions for LFV observables in the three different  $R\ell L$  models. Section IV briefly reviews the basic framework of RL and presents the BEs, upon which our numerical analysis is based. We also clarify the necessity of having at least three heavy Majorana neutrinos in RL models in order to obtain experimentally testable LFV. Section V presents numerical estimates of representative  $R\ell L$  models and their impact on the neutrino-mixing angle  $\theta_{13}$ . Finally, Sec. VI summarizes our conclusions.

## II. FLAVOR MODELS OF MINIMAL RESONANT LEPTOGENESIS

In this section, we describe the basic theoretical framework underlying the different flavor models of minimal RL. In particular, our interest is in scenarios in which the BAU is generated by the production of an individual lepton-number [13]. For definiteness, we first consider a minimal model for  $R\tau L$  in Sec. II A, and then generalize to the other two cases  $R\mu L$  and  $ReL$  in Secs. II B and II C, respectively.

The leptonic Yukawa and Majorana sectors of the SM symmetrically extended with one singlet right-handed neutrino  $\nu_{iR}$  per  $i$  family (with  $i = 1, 2, 3 = e, \mu, \tau$ ) are given by the Lagrangian

$$-\mathcal{L}_{Y,M} = \bar{L}\Phi\mathbf{h}^\ell l_R + \bar{L}\tilde{\Phi}\mathbf{h}^\nu\nu_R + \bar{\nu}_R^C\mathbf{m}_M\nu_R + \text{H.c.}, \quad (2.1)$$

where  $\Phi$  is the SM Higgs doublet and  $\tilde{\Phi} = i\tau_2\Phi^*$  its isospin conjugate. Moreover, we have suppressed the generation index  $i$  from the left-handed doublets  $L_i = (\nu_{iL}, l_{iL})^T$ , the right-handed charged leptons  $l_{iR}$  and the right-handed neutrinos  $\nu_{iR}$ , while ordinary multiplication between vectors and matrices is implied.<sup>1</sup>

To obtain a phenomenologically relevant model in this minimal setup, at least three singlet heavy Majorana neutrinos  $\nu_{1,2,3R}$  are needed and these have to be nearly degenerate in mass [13]. To ensure the latter, we assume that to leading order, the singlet Majorana sector is SO(3) symmetric, i.e.

$$\mathbf{m}_M = m_N\mathbf{1}_3 + \Delta\mathbf{m}_M, \quad (2.2)$$

where  $\mathbf{1}_3$  is the  $3 \times 3$  identity matrix and  $\Delta\mathbf{m}_M$  is a general SO(3)-breaking matrix induced by renormalization group (RG) effects. As we will discuss below, compatibility with the observed light-neutrino masses and mixings requires that  $(\Delta\mathbf{m}_M)_{ij}/m_N \lesssim 10^{-7}$ , for electroweak-mass Majorana neutrinos, i.e. for  $m_N \approx 0.1$ – $1$  TeV. We will explicitly demonstrate, how such an SO(3)-breaking matrix  $\Delta\mathbf{m}_M$ , of the required order, can be generated radiatively via the RG evolution of the right-handed neutrino mass matrix  $\mathbf{m}_M$  from the GUT-scale  $M_X \approx 2 \times 10^{16}$  GeV to the mass scale of the right-handed neutrinos  $m_N$ .

To one-loop order, the RG equations governing the  $3 \times 3$  matrices of the neutrino Yukawa couplings  $\mathbf{h}^\nu$ , the charged-lepton Yukawa couplings  $\mathbf{h}^\ell$  and the singlet Majorana-neutrino masses  $\mathbf{m}_M$  are given by [25]

$$\frac{d\mathbf{h}^\nu}{dt} = \frac{1}{16\pi^2} \left[ \left( \frac{9}{4}g_2^2 + \frac{3}{4}g_1^2 - T \right) \mathbf{1}_3 - \frac{3}{2}(\mathbf{h}^\nu\mathbf{h}^{\nu\dagger} - \mathbf{h}^\ell\mathbf{h}^{\ell\dagger}) \right] \mathbf{h}^\nu, \quad (2.3)$$

$$\frac{d\mathbf{h}^\ell}{dt} = \frac{1}{16\pi^2} \left[ \left( \frac{9}{4}g_2^2 + \frac{15}{4}g_1^2 - T \right) \mathbf{1}_3 + \frac{3}{2}(\mathbf{h}^\nu\mathbf{h}^{\nu\dagger} - \mathbf{h}^\ell\mathbf{h}^{\ell\dagger}) \right] \mathbf{h}^\ell, \quad (2.4)$$

$$\frac{d\mathbf{m}_M}{dt} = -\frac{1}{16\pi^2} [(\mathbf{h}^{\nu\dagger}\mathbf{h}^\nu)\mathbf{m}_M + \mathbf{m}_M(\mathbf{h}^{\nu T}\mathbf{h}^{\nu*})], \quad (2.5)$$

where  $t = \ln(M_X/\mu)$  and  $\mu$  is the RG evolution scale. Moreover,  $g_1$  and  $g_2$  are the gauge couplings of the  $U(1)_Y$  and  $SU(2)_L$  gauge groups, respectively, and  $T$  is the shorthand notation for the trace

$$T \equiv \text{Tr}(3\mathbf{h}^u\mathbf{h}^{u\dagger} + 3\mathbf{h}^d\mathbf{h}^{d\dagger} + \mathbf{h}^\nu\mathbf{h}^{\nu\dagger} + \mathbf{h}^\ell\mathbf{h}^{\ell\dagger}). \quad (2.6)$$

Here,  $\mathbf{h}^u$  and  $\mathbf{h}^d$  are the  $3 \times 3$  matrices for the up- and down-type Yukawa couplings, respectively. At the GUT scale  $M_X$ , we impose the universal boundary condition:  $\mathbf{m}_M(M_X) = m_N\mathbf{1}_3$ . The corresponding boundary values for

<sup>1</sup>Occasionally, we will also denote the individual lepton numbers with  $L_{e,\mu,\tau}$ , but hopefully the precise meaning of  $L_{e,\mu,\tau}$  can be easily inferred from the context, without causing confusion.

the neutrino Yukawa couplings  $\mathbf{h}^\nu$  depend on the particular model of  $R\ell L$ , which we now discuss in detail.

### A. Resonant $\tau$ -leptogenesis

In the physical charged-lepton mass basis, the  $SO(3)$  symmetry imposed on the singlet Majorana sector at the GUT scale  $M_X$  gets explicitly broken by a set of neutrino Yukawa couplings to the subgroup of lepton symmetries:  $U(1)_{L_e+L_\mu} \times U(1)_{L_\tau}$ . The flavor charge assignments that give rise to such a breaking are presented in Table I.

As a consequence of the  $U(1)_{L_e+L_\mu} \times U(1)_{L_\tau}$  symmetry, the neutrino Yukawa-coupling matrix takes on the general form:

$$\mathbf{h}^\nu = \begin{pmatrix} 0 & ae^{-i\pi/4} & ae^{i\pi/4} \\ 0 & be^{-i\pi/4} & be^{i\pi/4} \\ 0 & 0 & 0 \end{pmatrix} + \delta\mathbf{h}^\nu, \quad (2.7)$$

and  $\delta\mathbf{h}^\nu$  vanishes, if the symmetry is exact. In this symmetric limit, the light neutrinos remain massless to all orders in perturbation theory, while  $a$  and  $b$  are free unconstrained complex parameters. The phases accompanying these parameters in (2.7) are simply chosen for convenience to maximize the lepton asymmetry in leptogenesis (see Sec. IVA) when  $a$  and  $b$  are real. In order to give masses to the light neutrinos, the following minimal

TABLE I. Flavor charge assignments for the breaking  $SO(3) \rightarrow U(1)_{L_e+L_\mu} \times U(1)_{L_\tau}$ .

	$L_e, e_R$	$L_\mu, \mu_R$	$L_\tau, \tau_R$	$\nu_1$	$\nu_2 \pm i\nu_3$
$U(1)_{L_e+L_\mu}$	+1	+1	0	0	$\pm 1$
$U(1)_{L_\tau}$	0	0	+1	0	0

departure  $\delta\mathbf{h}^\nu$  from the flavor symmetric limit is considered:

$$\delta\mathbf{h}^\nu = \begin{pmatrix} \epsilon_e & 0 & 0 \\ \epsilon_\mu & 0 & 0 \\ \epsilon_\tau & \kappa_1 e^{-i(\pi/4-\gamma_1)} & \kappa_2 e^{i(\pi/4-\gamma_2)} \end{pmatrix}, \quad (2.8)$$

where  $|\epsilon_{e,\mu,\tau}|, \kappa_{1,2} \ll |a|, |b|$  and the phases  $\gamma_{1,2}$  are unrestricted. A more precise determination of the range of parameter values can be obtained from the low-energy neutrino data and successful leptogenesis.

It is important to notice that the flavor structure of the neutrino Yukawa couplings  $\mathbf{h}^\nu$  is preserved through the RG evolution, as long as  $\delta\mathbf{h}^\nu$  remains a small perturbation. In detail, RG effects violate the  $SO(3)$ -invariant form of the Majorana-mass matrix  $\mathbf{m}_M(M_X) = m_N \mathbf{1}_3$  by the  $3 \times 3$  matrix  $\Delta\mathbf{m}_M$ . In the leading-log approximation, the  $SO(3)$ -breaking matrix  $\Delta\mathbf{m}_M$  reads:

$$\Delta\mathbf{m}_M = -\frac{m_N}{8\pi^2} \ln\left(\frac{M_X}{m_N}\right) \text{Re}[\mathbf{h}^{\nu\dagger}(M_X)\mathbf{h}^\nu(M_X)] = -\frac{m_N}{8\pi^2} \ln\left(\frac{M_X}{m_N}\right) \times \begin{pmatrix} \epsilon_e^2 + \epsilon_\mu^2 + \epsilon_\tau^2 & \frac{1}{\sqrt{2}}(a\epsilon_e + b\epsilon_\mu) + \epsilon_\tau\kappa_1 \sin\bar{\gamma}_1 & \frac{1}{\sqrt{2}}(a\epsilon_e + b\epsilon_\mu) + \epsilon_\tau\kappa_2 \sin\bar{\gamma}_2 \\ \frac{1}{\sqrt{2}}(a\epsilon_e + b\epsilon_\mu) + \epsilon_\tau\kappa_1 \sin\bar{\gamma}_1 & a^2 + b^2 + \kappa_1^2 & \kappa_1\kappa_2 \sin(\gamma_1 + \gamma_2) \\ \frac{1}{\sqrt{2}}(a\epsilon_e + b\epsilon_\mu) + \epsilon_\tau\kappa_2 \sin\bar{\gamma}_2 & \kappa_1\kappa_2 \sin(\gamma_1 + \gamma_2) & a^2 + b^2 + \kappa_2^2 \end{pmatrix}, \quad (2.9)$$

with  $\bar{\gamma}_{1,2} = \gamma_{1,2} + \frac{\pi}{4}$ . Correspondingly, the neutrino and charged-lepton Yukawa couplings modify via RG running from  $M_X$  to  $m_N$  as follows:

$$\mathbf{h}^\nu(m_N) = \left[ \mathbf{1}_3 + \frac{\ln\left(\frac{M_X}{m_N}\right)}{16\pi^2} \begin{pmatrix} U - 3a^2 & -3ab & 0 \\ -3ab & U - 3b^2 & 0 \\ 0 & 0 & U + \frac{3}{2}h_\tau^2 \end{pmatrix} \right] \mathbf{h}^\nu(M_X), \quad (2.10)$$

$$\mathbf{h}^\ell(m_N) = \left[ \mathbf{1}_3 + \frac{\ln\left(\frac{M_X}{m_N}\right)}{16\pi^2} \begin{pmatrix} U' + 3a^2 & 3ab & 0 \\ 3ab & U' + 3b^2 & 0 \\ 0 & 0 & U' - \frac{3}{2}h_\tau^2 \end{pmatrix} \right] \mathbf{h}^\ell(M_X), \quad (2.11)$$

where  $U$  and  $U'$  stand for the shorthand expressions

$$U \equiv \frac{9}{4}g_2^2 + \frac{3}{4}g_1^2 - 3h_b^2 - 3h_t^2 - h_\tau^2 - 2a^2 - 2b^2, \quad U' \equiv \frac{9}{4}g_2^2 + \frac{15}{4}g_1^2 - 3h_b^2 - 3h_t^2 - h_\tau^2 - 2a^2 - 2b^2. \quad (2.12)$$

Observe that the universal contributions  $U$  and  $U'$  are dominated by the top-quark Yukawa coupling  $h_t$  and are approximately equal, i.e.  $U \approx U' \sim -3$ . For the models of interest to us, we have  $a, b, h_\tau \sim 10^{-2} \ll h_t$ , so the RG effects give rise to an overall rescaling of the charged and neutrino Yukawa couplings,  $\mathbf{h}^\ell$  and  $\mathbf{h}^\nu$ . Without loss of generality, we may assume that the charged-lepton Yukawa-coupling matrix  $\mathbf{h}^\ell$  is positive and diagonal at the scale  $m_N$ , i.e. close to the electroweak scale. Given the form invariance of  $\mathbf{h}^\nu$  under RG effects, we may therefore define all input parameters at the right-handed neutrino mass scale  $m_N$ , where the matching with the light-neutrino data is performed.

We may now determine the Yukawa parameters ( $a, b, \epsilon_e, \epsilon_\mu, \epsilon_\tau$ ), in terms of the light-neutrino mass matrix  $\mathbf{m}^\nu$  in the positive and diagonal charged-lepton Yukawa basis. To do so, we first notice that the chosen symmetry  $U(1)_{L_e+L_\mu} \times U(1)_{L_\tau}$  is sufficient to ensure the vanishing of the light-neutrino mass matrix  $\mathbf{m}^\nu$ . In fact, if it is an exact symmetry of the theory, the light-neutrino mass matrix will vanish to all orders in perturbation theory [26]. To leading order in the symmetry-breaking parameters  $\Delta\mathbf{m}_M$  and  $\delta\mathbf{h}^\nu$ , the tree-level light-neutrino mass matrix  $\mathbf{m}^\nu$  is given by

$$\begin{aligned} \mathbf{m}^\nu &= -\frac{v^2}{2} \mathbf{h}^\nu \mathbf{m}_M^{-1} \mathbf{h}^{\nu T} = \frac{v^2}{2m_N} \left( \frac{\mathbf{h}^\nu \Delta\mathbf{m}_M \mathbf{h}^{\nu T}}{m_N} - \mathbf{h}^\nu \mathbf{h}^{\nu T} \right) \\ &= -\frac{v^2}{2m_N} \begin{pmatrix} \frac{\Delta m_N}{m_N} a^2 - \epsilon_e^2 & \frac{\Delta m_N}{m_N} ab - \epsilon_e \epsilon_\mu & -\epsilon_e \epsilon_\tau \\ \frac{\Delta m_N}{m_N} ab - \epsilon_e \epsilon_\mu & \frac{\Delta m_N}{m_N} b^2 - \epsilon_\mu^2 & -\epsilon_\mu \epsilon_\tau \\ -\epsilon_e \epsilon_\tau & -\epsilon_\mu \epsilon_\tau & -\epsilon_\tau^2 \end{pmatrix}, \end{aligned} \quad (2.13)$$

where  $v = 2M_W/g_w = 245$  GeV is the vacuum expectation value of the SM Higgs field  $\Phi$ . In deriving the last equation in (2.13), we have also assumed that  $\sqrt{\frac{\Delta m_N}{m_N}} \kappa_{1,2} \ll \epsilon_{e,\mu,\tau}$ , where  $\Delta m_N$  stands for the expression

$$\begin{aligned} \Delta m_N &\equiv 2(\Delta\mathbf{m}_M)_{23} + i[(\Delta\mathbf{m}_M)_{33} - (\Delta\mathbf{m}_M)_{22}] \\ &= -\frac{m_N}{8\pi^2} \ln\left(\frac{M_X}{m_N}\right) [2\kappa_1 \kappa_2 \sin(\gamma_1 + \gamma_2) \\ &\quad + i(\kappa_2^2 - \kappa_1^2)]. \end{aligned} \quad (2.14)$$

As a consequence of the flavor symmetry  $U(1)_{L_e+L_\mu} \times U(1)_{L_\tau}$ , the symmetry-violating parameters  $\epsilon_{e,\mu,\tau}$  and  $\kappa_{1,2}$  enter the tree-level light-neutrino mass matrix  $\mathbf{m}^\nu$  in (2.13) quadratically. This in turn implies that for electroweak-scale heavy neutrinos  $m_N \sim v$ , the symmetry-breaking Yukawa couplings  $\delta\mathbf{h}^\nu$  in (2.8) need not be much smaller than the electron Yukawa coupling  $h_e \sim 10^{-6}$ . Moreover, one should observe that only a particular combination of SO(3)-violating terms  $(\Delta\mathbf{m}_M)_{ij}$  appears in  $\mathbf{m}^\nu$  through  $\Delta m_N$ . Nevertheless, for electroweak-scale heavy neutrinos

with mass differences  $|\Delta m_N|/m_N \lesssim 10^{-7}$ , one should have  $|a|, |b| \lesssim 10^{-2}$  to avoid getting too large light-neutrino masses much above 0.5 eV.

Given the analytic form (2.13) of the light-neutrino mass matrix, we may directly compute the neutrino Yukawa couplings ( $a, b, \epsilon_e, \epsilon_\mu, \epsilon_\tau$ ), as functions of  $m_N$ , the phenomenologically constrained neutrino mass matrix  $\mathbf{m}^\nu$  and the symmetry-breaking parameters  $\kappa_{1,2}$  and  $\gamma_{1,2}$ :

$$\begin{aligned} a^2 &= \frac{2m_N}{v^2} \frac{8\pi^2}{\ln(M_X/m_N)} \left( m_{11}^\nu - \frac{(m_{13}^\nu)^2}{m_{33}^\nu} \right) \\ &\quad \times [2\kappa_1 \kappa_2 \sin(\gamma_1 + \gamma_2) + i(\kappa_2^2 - \kappa_1^2)]^{-1}, \\ b^2 &= \frac{2m_N}{v^2} \frac{8\pi^2}{\ln(M_X/m_N)} \left( m_{22}^\nu - \frac{(m_{23}^\nu)^2}{m_{33}^\nu} \right) \\ &\quad \times [2\kappa_1 \kappa_2 \sin(\gamma_1 + \gamma_2) + i(\kappa_2^2 - \kappa_1^2)]^{-1}, \quad (2.15) \\ \epsilon_e^2 &= \frac{2m_N}{v^2} \frac{(m_{13}^\nu)^2}{m_{33}^\nu}, \\ \epsilon_\mu^2 &= \frac{2m_N}{v^2} \frac{(m_{23}^\nu)^2}{m_{33}^\nu}, \\ \epsilon_\tau^2 &= \frac{2m_N}{v^2} m_{33}^\nu. \end{aligned}$$

Since the approximate light-neutrino mass matrix  $\mathbf{m}^\nu$  in (2.13) has rank two, the lightest neutrino mass eigenstate  $\nu_1$  will be massless in this approximation. The relations given in (2.15) will be used to obtain numerical estimates of the BAU, in terms of  $m_N$  and the symmetry-breaking parameters  $\kappa_{1,2}$  and  $\gamma_{1,2}$ , for both normal and inverted hierarchy scenarios of light neutrinos. In the following, we discuss the two remaining flavor variants of RL: R $\mu$ L and ReL.

## B. Resonant $\mu$ -leptogenesis

The flavor scenario of R $\mu$ L gets realized, once the GUT-scale SO(3) symmetry gets broken to  $U(1)_{L_e+L_\tau} \times U(1)_{L_\mu}$ . The flavor charge assignments related to this breaking are presented in Table II. As a consequence, the neutrino Yukawa coupling  $\mathbf{h}^\nu$  takes on the form:

$$\mathbf{h}^\nu = \begin{pmatrix} 0 & ae^{-i\pi/4} & ae^{i\pi/4} \\ 0 & 0 & 0 \\ 0 & be^{-i\pi/4} & be^{i\pi/4} \end{pmatrix} + \delta\mathbf{h}^\nu, \quad (2.16)$$

TABLE II. Flavor charge assignments for the breaking  $SO(3) \rightarrow U(1)_{L_e+L_\tau} \times U(1)_{L_\mu}$ .

	$L_e, e_R$	$L_\mu, \mu_R$	$L_\tau, \tau_R$	$\nu_1$	$\nu_2 \pm i\nu_3$
$U(1)_{L_e+L_\tau}$	+1	0	+1	0	$\pm 1$
$U(1)_{L_\mu}$	0	+1	0	0	0



where the subdominant neutrino Yukawa-coupling matrix,

$$\delta \mathbf{h}^\nu = \begin{pmatrix} \epsilon_e & 0 & 0 \\ \epsilon_\mu & \kappa_1 e^{-i(\pi/4-\gamma_1)} & \kappa_2 e^{i(\pi/4-\gamma_2)} \\ \epsilon_\tau & 0 & 0 \end{pmatrix}, \quad (2.17)$$

breaks minimally the  $U(1)_{L_e+L_\tau} \times U(1)_{L_\mu}$  flavor symmetry.

As in the R $\tau$ L case, we assume that the Majorana mass matrix  $\mathbf{m}_M$  is proportional to  $\mathbf{1}_3$  at the GUT scale  $M_X$  and gets radiatively broken via RG effects at the heavy-Majorana-neutrino scale  $m_N$ . Taking into account both symmetry-breaking terms  $\Delta \mathbf{m}_M$  and  $\delta \mathbf{h}^\nu$ , the light-neutrino mass matrix acquires an analogous form in R $\mu$ L :

$$\mathbf{m}^\nu = -\frac{v^2}{2m_N} \times \begin{pmatrix} \frac{\Delta m_N}{m_N} a^2 - \epsilon_e^2 & -\epsilon_e \epsilon_\mu & \frac{\Delta m_N}{m_N} ab - \epsilon_e \epsilon_\tau \\ -\epsilon_e \epsilon_\mu & -\epsilon_\mu^2 & -\epsilon_\mu \epsilon_\tau \\ \frac{\Delta m_N}{m_N} ab - \epsilon_e \epsilon_\tau & -\epsilon_\mu \epsilon_\tau & \frac{\Delta m_N}{m_N} b^2 - \epsilon_\tau^2 \end{pmatrix}, \quad (2.18)$$

where  $\Delta m_N$  is given by (2.14). Correspondingly, the neutrino Yukawa-coupling parameters ( $a, b, \epsilon_e, \epsilon_\mu, \epsilon_\tau$ ) may be analogously expressed, in terms of  $\mathbf{m}^\nu, m_N, \kappa_{1,2}$  and  $\gamma_{1,2}$  as follows:

$$\begin{aligned} a^2 &= \frac{2m_N}{v^2} \frac{8\pi^2}{\ln(M_X/m_N)} \left( m_{11}^\nu - \frac{(m_{12}^\nu)^2}{m_{22}^\nu} \right) \\ &\quad \times [2\kappa_1 \kappa_2 \sin(\gamma_1 + \gamma_2) + i(\kappa_2^2 - \kappa_1^2)]^{-1}, \\ b^2 &= \frac{2m_N}{v^2} \frac{8\pi^2}{\ln(M_X/m_N)} \left( m_{33}^\nu - \frac{(m_{23}^\nu)^2}{m_{22}^\nu} \right) \\ &\quad \times [2\kappa_1 \kappa_2 \sin(\gamma_1 + \gamma_2) + i(\kappa_2^2 - \kappa_1^2)]^{-1}, \\ \epsilon_e^2 &= \frac{2m_N}{v^2} \frac{(m_{12}^\nu)^2}{m_{22}^\nu}, \\ \epsilon_\mu^2 &= \frac{2m_N}{v^2} m_{22}^\nu, \\ \epsilon_\tau^2 &= \frac{2m_N}{v^2} \frac{(m_{23}^\nu)^2}{m_{22}^\nu}. \end{aligned} \quad (2.19)$$

### C. Resonant $e$ -leptogenesis

A third possible flavor scenario pertinent to ReL is realized by the symmetry-breaking pattern  $SO(3) \rightarrow U(1)_{L_\mu+L_\tau} \times U(1)_{L_e}$ , where the flavor charge assignments are given in Table III. In ReL, the neutrino Yukawa coupling  $\mathbf{h}^\nu$  has the structure:

TABLE III. Flavor charge assignments for the breaking  $SO(3) \rightarrow U(1)_{L_\mu+L_\tau} \times U(1)_{L_e}$ .

	$L_e, e_R$	$L_\mu, \mu_R$	$L_\tau, \tau_R$	$\nu_1$	$\nu_2 \pm i\nu_3$
$U(1)_{L_\mu+L_\tau}$	0	+1	+1	0	$\pm 1$
$U(1)_{L_e}$	+1	0	0	0	0

$$\mathbf{h}^\nu = \begin{pmatrix} 0 & 0 & 0 \\ 0 & ae^{-i\pi/4} & ae^{i\pi/4} \\ 0 & be^{-i\pi/4} & be^{i\pi/4} \end{pmatrix} + \delta \mathbf{h}^\nu, \quad (2.20)$$

and the breaking terms  $\delta \mathbf{h}^\nu$  of the  $U(1)_{L_\mu+L_\tau} \times U(1)_{L_e}$  flavor symmetry are

$$\delta \mathbf{h}^\nu = \begin{pmatrix} \epsilon_e & \kappa_1 e^{-i(\pi/4-\gamma_1)} & \kappa_2 e^{i(\pi/4-\gamma_2)} \\ \epsilon_\mu & 0 & 0 \\ \epsilon_\tau & 0 & 0 \end{pmatrix}. \quad (2.21)$$

In close analogy with the previous two scenarios of R $\tau$ L and R $\mu$ L, the light-neutrino mass matrix in ReL is given by

$$\mathbf{m}^\nu = -\frac{v^2}{2m_N} \begin{pmatrix} -\epsilon_e^2 & -\epsilon_e \epsilon_\mu & -\epsilon_e \epsilon_\tau \\ -\epsilon_e \epsilon_\mu & \frac{\Delta m_N}{m_N} a^2 - \epsilon_\mu^2 & \frac{\Delta m_N}{m_N} ab - \epsilon_\mu \epsilon_\tau \\ -\epsilon_e \epsilon_\tau & \frac{\Delta m_N}{m_N} ab - \epsilon_\mu \epsilon_\tau & \frac{\Delta m_N}{m_N} b^2 - \epsilon_\tau^2 \end{pmatrix}, \quad (2.22)$$

where  $\Delta m_N$  retains its analytic form of (2.14). By analogy, we may derive in ReL the relations of the neutrino Yukawa-coupling parameters ( $a, b, \epsilon_e, \epsilon_\mu, \epsilon_\tau$ ) to  $\mathbf{m}^\nu, m_N, \kappa_{1,2}$  and  $\gamma_{1,2}$ . These are given by

$$\begin{aligned} a^2 &= \frac{2m_N}{v^2} \frac{8\pi^2}{\ln(M_X/m_N)} \left( m_{22}^\nu - \frac{(m_{12}^\nu)^2}{m_{11}^\nu} \right) \\ &\quad \times [2\kappa_1 \kappa_2 \sin(\gamma_1 + \gamma_2) + i(\kappa_2^2 - \kappa_1^2)]^{-1}, \\ b^2 &= \frac{2m_N}{v^2} \frac{8\pi^2}{\ln(M_X/m_N)} \left( m_{33}^\nu - \frac{(m_{13}^\nu)^2}{m_{11}^\nu} \right) \\ &\quad \times [2\kappa_1 \kappa_2 \sin(\gamma_1 + \gamma_2) + i(\kappa_2^2 - \kappa_1^2)]^{-1}, \\ \epsilon_e^2 &= \frac{2m_N}{v^2} m_{11}^\nu, \\ \epsilon_\mu^2 &= \frac{2m_N}{v^2} \frac{(m_{12}^\nu)^2}{m_{11}^\nu}, \\ \epsilon_\tau^2 &= \frac{2m_N}{v^2} \frac{(m_{13}^\nu)^2}{m_{11}^\nu}. \end{aligned} \quad (2.23)$$

### III. LOW-ENERGY OBSERVABLES

Low-energy neutrino data provide indisputable evidence for neutrino oscillations. We use these data to determine and constrain the fundamental parameters of the theory. We also present the full range of predictions for the half life

of neutrinoless double-beta decay of a heavy nucleus, within the different flavor scenarios of RL. In the same context, we present analytic results and estimates for LFV observables, such as  $\mu \rightarrow e\gamma$  and  $\mu \rightarrow e$  conversion in nuclei.

### A. Light-neutrino oscillation data

The interpretation of the experimental results on solar neutrinos suggests that  $\nu_e \rightarrow \nu_{\mu,\tau}$  oscillations are mainly driven by the mass squared difference  $\Delta m_{12}^2 = m_{\nu_2}^2 - m_{\nu_1}^2$ , while the corresponding experimental data on atmospheric neutrinos are interpreted by  $\nu_\mu \rightarrow \nu_\tau$  oscillations driven by  $\Delta m_{23}^2 = m_{\nu_3}^2 - m_{\nu_2}^2$ , within a minimal scheme of three active neutrinos. For the present analysis, we use the global fits performed in [27], even though global fits of other groups give compatible results [28]. The best fit values for the light-neutrino masses and mixings, including their uncertainties at the  $2\sigma$  level, are given by

$$\begin{aligned} \sin^2\theta_{12} &= 0.32_{-0.04}^{+0.05}, \\ \sin^2\theta_{23} &= 0.50_{-0.12}^{+0.13}, \\ \sin^2\theta_{13} &= 0.007_{-0.007}^{+0.026}, \\ \Delta m_{12}^2 &= (7.6_{-0.3}^{+0.5}) \times 10^{-5} \text{ eV}^2, \\ |\Delta m_{13}^2| &= (2.4_{-0.3}^{+0.3}) \times 10^{-3} \text{ eV}^2, \end{aligned} \quad (3.1)$$

where the sign of  $\Delta m_{13}^2 \equiv \Delta m_{12}^2 + \Delta m_{23}^2$  remains still undetermined, corresponding to the cases of the so-called normal ( $\Delta m_{13}^2 > 0$ ) and inverted ( $\Delta m_{13}^2 < 0$ ) neutrino mass hierarchy, respectively. As outlined in Sec. II, we use the oscillation parameters as input to reduce the number of free parameters in the neutrino Yukawa-coupling matrix  $\mathbf{h}^\nu$ .

### B. $0\nu\beta\beta$ decay

Models that include Majorana neutrinos violate the  $L$ -number and so can give rise to neutrinoless double-beta decay ( $0\nu\beta\beta$ ) of a heavy nucleus  ${}^A_Z X$ , where two single  $\beta$  decays [29–31] can occur simultaneously in one nucleus,  ${}^A_Z X \rightarrow {}^A_{Z+2} X + 2e^-$ . The measurement of the half-life of this decay provides further information on the structure of the light-neutrino mass matrix  $\mathbf{m}^\nu$ . The half-life  $T_{1/2}^{0\nu\beta\beta}$  for a  $0\nu\beta\beta$  decay mediated by light Majorana neutrinos is given by

$$(T_{1/2}^{0\nu\beta\beta})^{-1} = \frac{\langle m \rangle^2}{m_e^2} |\mathcal{M}_{0\nu\beta\beta}|^2 G_{01}, \quad (3.2)$$

where  $\langle m \rangle$  denotes the effective Majorana-neutrino mass,  $m_e$  is the electron mass and  $\mathcal{M}_{0\nu\beta\beta}$  and  $G_{01}$  are the nuclear matrix element and the phase space factor of the decay, respectively. The effective neutrino mass  $\langle m \rangle$  is given by the entry  $\{11\} \equiv \{ee\}$  of the light-neutrino mass matrix  $\mathbf{m}^\nu$ , which can be expressed as

$$\langle m \rangle \equiv |\mathbf{m}_{ee}^\nu| = \left| \sum_{i=1}^3 (U_{ei}^\nu)^2 m_{\nu_i} \right|, \quad (3.3)$$

where  $U^\nu$  is the Pontecorvo-Maki-Nakagawa-Sakata neutrino-mixing matrix [32]. As described in Sec. II, RL models realize a light-neutrino mass spectrum with a vanishing lightest neutrino mass,  $m_{\nu_1} = 0$ , and either a normal or inverted mass hierarchy. The prediction for the effective Majorana-neutrino mass for these two scenarios is given by

$$\langle m \rangle = \begin{cases} (2.5_{-2.5}^{+3.0}) \times 10^{-3} & \Delta m_{13}^2 > 0 \\ (2.9_{-1.9}^{+3.0}) \times 10^{-2} & \Delta m_{13}^2 < 0 \end{cases}. \quad (3.4)$$

The above prediction takes into account the uncertainty of the observed oscillation parameters at the  $2\sigma$  level and the variation of the unknown Dirac and Majorana phases. These predictions are to be compared to the experimental bound  $T_{1/2}^{0\nu\beta\beta} > 1.9 \times 10^{25}$  years in the isotope  ${}^{76}\text{Ge}$  reported by the Heidelberg–Moscow collaboration [33], implying an upper limit on  $\langle m \rangle$  in the range:

$$\langle m \rangle_{\text{exp}} < (0.3\text{--}0.6) \text{ eV}. \quad (3.5)$$

Here, the main uncertainty is due to the choice for the nuclear matrix element that occurs in (3.2). Future  $0\nu\beta\beta$ -decay experiments are expected to probe  $\langle m \rangle$  to sensitivities of order  $10^{-2}$  [19] and so fall within the range given in (3.4) to validate the mass scenario of inverted hierarchy.

### C. $l_1 \rightarrow l_2\gamma$

Heavy Majorana-neutrino loop effects may induce sizeable LFV couplings to the photon and the  $Z$  boson. These couplings give rise to LFV decays, such as  $\mu \rightarrow e\gamma$  [34],  $\mu \rightarrow eee$  [35] and  $\mu \rightarrow e$  conversion in nuclei. The strength of LFV is controlled by the effective coupling matrix

$$\mathbf{\Omega}_{l_1 l_2} = \frac{v^2}{2m_N^2} (\mathbf{h}^\nu \mathbf{h}^{\nu\dagger})_{l_1 l_2}, \quad (3.6)$$

which governs the flavor transition between the charged leptons  $l_{1,2} = e, \mu, \tau$  in LFV processes. The LFV decay  $l_1 \rightarrow l_2\gamma$ ,  $l_1 \in \{\mu, \tau\}$ , with  $l_2 \in \{\mu, e\}$ ,  $l_2 \neq l_1$ , whose branching fraction is given by

$$B(l_1 \rightarrow l_2\gamma) = \frac{\alpha_w^3 s_w^2}{256\pi^2} \frac{m_{l_1}^4}{M_W^4} \frac{m_{l_1}}{\Gamma_{l_1}} |G_\gamma^{l_1 l_2}|^2. \quad (3.7)$$

In the above,  $\Gamma_{l_1}$  is the decay width of lepton  $l_1$  and  $G_\gamma^{\mu e}$  is a composite form-factor given by [35]

$$G_\gamma^{l_1 l_2} = -\mathbf{\Omega}_{l_1 l_2} G_\gamma \left( \frac{m_N^2}{m_W^2} \right), \quad (3.8)$$

with

$$G_\gamma(x) = -\frac{2x^3 + 5x^2 - x}{4(1-x)^3} - \frac{3x^3}{2(1-x)^4} \ln x. \quad (3.9)$$

Given that the experimentally measured muon and tau decay widths are  $\Gamma_\mu = 2.997 \times 10^{-19}$  GeV and  $\Gamma_\tau = 2.158 \times 10^{-12}$  GeV [36], the LFV branching ratios can be expressed as

$$B(\mu \rightarrow e\gamma) \approx 8.0 \cdot 10^{-4} \times g\left(\frac{m_N}{m_W}\right) |\Omega_{\mu e}|^2, \quad (3.10)$$

$$B(\tau \rightarrow l_2\gamma) \approx 1.5 \cdot 10^{-4} \times g\left(\frac{m_N}{m_W}\right) |\Omega_{\tau l_2}|^2, \quad l_2 = e, \mu. \quad (3.11)$$

Here, we defined  $g(x) \equiv 4G_\gamma^2(x^2)$ , which possesses the limits  $g \rightarrow 1$  for  $m_N \gg m_W$  and  $g \rightarrow 1/16$  for  $m_N = m_W$ . Our theoretical predictions will be contrasted to the current experimental upper limits [36]

$$\begin{aligned} B_{\text{exp}}(\mu \rightarrow e\gamma) &< 1.2 \times 10^{-11}, \\ B_{\text{exp}}(\tau \rightarrow \mu\gamma) &< 6.8 \times 10^{-8}, \\ B_{\text{exp}}(\tau \rightarrow e\gamma) &< 1.1 \times 10^{-7}, \end{aligned} \quad (3.12)$$

and the expected sensitivity of the MEG experiment [20],

$$B_{\text{MEG}}(\mu \rightarrow e\gamma) \approx 10^{-13}. \quad (3.13)$$

In R $\ell$ L models, only two of the right-handed neutrinos,  $\nu_{2R}$  and  $\nu_{3R}$ , have appreciable  $e$ - and  $\mu$ -Yukawa couplings,  $a, b \approx 10^{-2}$ ,  $\kappa_{1,2} = 10^{-5}$ – $10^{-3}$ , and will be relevant to LFV effects. For example, in the R $\tau$ L model, the parameters  $|\Omega_{l_1 l_2}|^2$  are, to a good approximation, given by

$$\begin{aligned} |\Omega_{\mu e}|^2 &\approx \frac{v^4}{m_N^4} a^2 b^2, \\ |\Omega_{\tau \mu}|^2 &\approx \frac{v^4}{m_N^4} \max(\kappa_1^2, \kappa_2^2) b^2, \\ |\Omega_{\tau e}|^2 &\approx \frac{v^4}{m_N^4} \max(\kappa_1^2, \kappa_2^2) a^2. \end{aligned} \quad (3.14)$$

Because of the relations (2.15),  $a$  and  $b$  are approximately inversely proportional to  $\kappa_{1,2}$ ,  $a, b \approx 3 \times 10^{-7} \kappa_{1,2}^{-1}$  (in the case of a normal light-neutrino mass hierarchy), and for a typical value of  $\kappa_{1,2} \approx 10^{-4}$ ,  $a$  and  $b$  are of the order  $a, b \approx 3 \times 10^{-3}$ . Thus, in the R $\tau$ L scenario, the following typical values for the branching ratios of the photonic LFV  $\mu$  and  $\tau$  decays are predicted:

$$B(\mu \rightarrow e\gamma)_{R\tau L} \approx 10^{-13}, \quad B(\tau \rightarrow l_2\gamma)_{R\tau L} \approx 10^{-17}. \quad (3.15)$$

Consequently, only  $B(\mu \rightarrow e\gamma)$  is expected to be within reach of future experiments, whereas the LFV  $\tau$  decays are far beyond the realm of detection. By analogy, the predictions in the  $Re(\mu)L$  model are found to be

$$\begin{aligned} B(\mu \rightarrow e\gamma)_{Re(\mu)L} &\approx 10^{-16}, \\ B(\tau \rightarrow l_2\gamma)_{Re(\mu)L} &\approx 10^{-14}. \end{aligned} \quad (3.16)$$

Again,  $B(\tau \rightarrow \mu\gamma)$  and  $B(\tau \rightarrow e\gamma)$  are expected to be below current and future experimental sensitivities for parameter choices compatible with successful leptogenesis. While the prediction for  $B(\mu \rightarrow e\gamma)$  is far below the expected MEG sensitivity, the LFV  $\mu \rightarrow e$  transition rate might still be high enough to be testable at future experiments measuring  $\mu \rightarrow e$  conversion in nuclei (see next section). Because of the inverse proportionality between  $a, b$  and  $\kappa_{1,2}$  the prediction for  $B(\mu \rightarrow e\gamma)$  is essentially independent of the choice for  $\kappa_{1,2}$ . In Sec. V, we present detailed numerical results for LFV  $\mu$ - and  $\tau$ -decays that confirm the validity of these simple estimates.

### D. Coherent $\mu \rightarrow e$ conversion in nuclei

One of the most sensitive probes of LFV is the coherent conversion of  $\mu \rightarrow e$  in nuclei [37,38]. The  $\mu \rightarrow e$  conversion rate in a nucleus with nucleon numbers  $(N, Z)$  is given by [37–39]

$$\begin{aligned} B_{\mu e}(N, Z) &\equiv \frac{\Gamma[\mu(N, Z) \rightarrow e(N, Z)]}{\Gamma[\mu(N, Z) \rightarrow \text{capture}]} \\ &\approx \frac{\alpha_{\text{em}}^3 \alpha_w^4 m_\mu^5}{16\pi^2 m_W^4 \Gamma_{\text{capt}}} \frac{Z_{\text{eff}}^4}{Z} |F(-m_\mu^2)|^2 |Q_W|^2, \end{aligned} \quad (3.17)$$

where  $\alpha_{\text{em}} = 1/137$  is the electromagnetic fine structure constant,  $Z_{\text{eff}}$  is the effective atomic number and  $\Gamma_{\text{capt}}$  is the muon nuclear capture rate. For  ${}^{48}_{22}\text{Ti}$ , experimental measurements give  $Z_{\text{eff}} \approx 17.6$  [40] and  $\Gamma_{\text{capt}} \approx 1.705 \times 10^{-18}$  GeV [41]. Moreover,  $|F(-m_\mu^2)| \approx 0.54$  is the nuclear form factor [42] and

$$Q_W = V_u(2Z + N) + V_d(Z + 2N) \quad (3.18)$$

is the weak matrix element, where

$$\begin{aligned} V_u &= -\left[1 + \frac{1}{3}s_w^2 + \left(\frac{3}{8} - \frac{8}{9}s_w^2\right) \ln \frac{m_N^2}{m_W^2}\right] \Omega_{\mu e} \\ &\quad + \frac{1}{2} \left(\frac{1}{4} + \frac{2}{3}s_w^2\right) \frac{m_N^2}{m_W^2} (\Omega^2)_{\mu e}, \end{aligned} \quad (3.19)$$

$$\begin{aligned} V_d &= \left[\frac{1}{4} + \frac{1}{6}s_w^2 + \left(\frac{3}{8} - \frac{4}{9}s_w^2\right) \ln \frac{m_N^2}{m_W^2}\right] \Omega_{\mu e} \\ &\quad + \frac{1}{2} \left(\frac{1}{4} + \frac{1}{3}s_w^2\right) \frac{m_N^2}{m_W^2} (\Omega^2)_{\mu e}. \end{aligned} \quad (3.20)$$

In the case of  ${}^{48}_{22}\text{Ti}$ ,  $B_{\mu e}(26, 22)$  is then approximately related to  $B(\mu \rightarrow e\gamma)$  through

$$B_{\mu e}(26, 22) \approx 10^{-1} \times B(\mu \rightarrow e\gamma), \quad (3.21)$$

for a right-handed neutrino mass scale  $m_N \approx 100$  GeV. On the experimental side, the strongest upper bound

is obtained from data on  $\mu \rightarrow e$  conversion in  $^{48}_{22}\text{Ti}$  [43],

$$B_{\mu e}^{\text{exp}}(26, 22) < 4.3 \times 10^{-12}. \quad (3.22)$$

Using the relation (3.21), we observe that this sensitivity is comparable to the current bound on  $B(\mu \rightarrow e\gamma)$ . However, the proposed COMET and mu2e experiments, measuring  $\mu \rightarrow e$  conversion in  $^{27}_{13}\text{Al}$ , are expected to be sensitive to conversion rates of order  $10^{-16}$  [44,45], thereby improving the sensitivity compared to the current limit by 4 orders of magnitude.

#### IV. LEPTOGENESIS

In this section, we briefly review the central results of the field-theoretic formalism for RL developed in [7,8] which will be used in our analysis. We then set up the BEs and present approximate solutions for the kinematic regime of interest to us. Finally, we clarify the necessity of introducing at least three right-handed neutrinos into the theory, in order to explain the BAU and obtain testable rates of LFV, such as  $B(\mu \rightarrow e\gamma) \sim 10^{-12} - 10^{-13}$ .

##### A. Leptonic asymmetries

Within the framework of leptogenesis, a net nonzero leptonic asymmetry results from the  $CP$ -violating decays of the heavy Majorana neutrinos  $N_\alpha$  into the left-handed charged leptons  $l_L^-$  and light neutrinos  $\nu_{lL}$ . Consequently, we have to calculate the partial decay width of the heavy Majorana neutrino  $N_\alpha$  into a particular lepton flavor  $l$ ,

$$\Gamma_{\alpha l} = \Gamma(N_\alpha \rightarrow l_L^- + W^+) + \Gamma(N_\alpha \rightarrow \nu_{lL} + Z, H). \quad (4.1)$$

$$\begin{aligned} \bar{\mathbf{h}}_{l\alpha}^\nu(\mathbf{h}^\nu) &= \mathbf{h}_{l\alpha}^\nu - i \sum_{\beta, \gamma=1}^3 |\varepsilon_{\alpha\beta\gamma}| \mathbf{h}_{l\beta}^\nu \\ &\times \frac{m_\alpha(m_\alpha A_{\alpha\beta} + m_\beta A_{\beta\alpha}) - iR_{\alpha\gamma}[m_\alpha A_{\gamma\beta}(m_\alpha A_{\alpha\gamma} + m_\gamma A_{\gamma\alpha}) + m_\beta A_{\beta\gamma}(m_\alpha A_{\gamma\alpha} + m_\gamma A_{\alpha\gamma})]}{m_\alpha^2 - m_\beta^2 + 2im_\alpha^2 A_{\beta\beta} + 2i \text{Im}R_{\alpha\gamma}(m_\alpha^2 |A_{\beta\gamma}|^2 + m_\beta m_\gamma \text{Re}A_{\beta\gamma}^2)}, \end{aligned} \quad (4.4)$$

where  $|\varepsilon_{\alpha\beta\gamma}|$  is the modulus of the usual Levi-Civita antisymmetric tensor ( $\varepsilon_{123} = 1$ ),  $m_\alpha^2 \equiv m_{N_\alpha}^2$ ,  $A_{\alpha\beta} \equiv A_{\alpha\beta}(\mathbf{h}^\nu)$  and

$$R_{\alpha\beta} = \frac{m_\alpha^2}{m_\alpha^2 - m_\beta^2 + 2im_\alpha^2 A_{\beta\beta}}. \quad (4.5)$$

The respective  $CP$ -conjugate effective Yukawa couplings  $\bar{\mathbf{h}}_{l\alpha}^{\nu C}(\mathbf{h}^\nu)$  are obtained from (4.4) by replacing the tree-level couplings  $\mathbf{h}_{l\alpha}^\nu$  with their complex conjugates  $\mathbf{h}_{l\alpha}^{\nu*}$ :

$$\bar{\mathbf{h}}_{l\alpha}^{\nu C}(\mathbf{h}^\nu) = \bar{\mathbf{h}}_{l\alpha}^\nu(\mathbf{h}^{\nu*}). \quad (4.6)$$

For temperatures above the electroweak phase transition, the SM vacuum expectation value vanishes and only the would-be Goldstone and Higgs modes will predominantly contribute to  $\Gamma_{\alpha l}$ .

In RL models, resumming the absorptive parts of the heavy Majorana-neutrino self-energy transitions  $N_\beta \rightarrow N_\alpha$  plays an important role in the computation of  $\Gamma_{\alpha l}$  [7,8]. In order to take this resummation consistently into account, we first introduce the lepton-flavor dependent absorptive transition amplitude [46]

$$A_{\alpha\beta}^l(\mathbf{h}^\nu) \equiv \frac{\mathbf{h}_{l\alpha}^\nu \mathbf{h}_{l\beta}^{\nu*}}{16\pi}, \quad (4.2)$$

which represents the contribution of a single charged lepton and light-neutrino flavor  $l$  running in the loop. Summing over all flavors  $l$ , we then get the total transition amplitude

$$A_{\alpha\beta}(\mathbf{h}^\nu) \equiv \sum_{l=e,\mu,\tau} A_{\alpha\beta}^l(\mathbf{h}^\nu) = \frac{(\mathbf{h}^{\nu\dagger} \mathbf{h}^\nu)_{\alpha\beta}^*}{16\pi}. \quad (4.3)$$

Note that the diagonal transition amplitude  $A_{\alpha\alpha}$  is related to the tree-level decay width of the heavy Majorana neutrino  $N_\alpha$  through:  $\Gamma_{N_\alpha}^{(0)} = 2m_{N_\alpha} A_{\alpha\alpha}(\mathbf{h}^\nu)$ .

Since all charged-lepton Yukawa couplings will be in thermal equilibrium in the low-scale leptogenesis scenarios of our interest, we consider the weak basis in which the matrices  $\mathbf{h}^\ell$  and  $\mathbf{m}_M$  are both diagonal and positive. To account for unstable-particle mixing effects between the three heavy Majorana neutrinos, we follow [7,8] and define the resummed effective Yukawa couplings  $\bar{\mathbf{h}}_{l\alpha}^\nu$  and their  $CP$ -conjugate ones  $\bar{\mathbf{h}}_{l\alpha}^{\nu C}$  related to the vertices  $L\tilde{\Phi}N_\alpha$  and  $L^C\tilde{\Phi}^*N_\alpha$ , respectively. The resummed neutrino Yukawa couplings  $\bar{\mathbf{h}}_{l\alpha}^\nu$  are given by [8,46]

In our calculations, we neglect the one-loop corrections to the proper vertices  $L\tilde{\Phi}N_\alpha$ , whose absorptive parts are numerically insignificant in RL. In terms of the absorptive transition amplitudes  $A_{\alpha\beta}^l$  given in (4.2), the partial decay widths  $\Gamma_{\alpha l}$  and their  $CP$ -conjugates  $\Gamma_{\alpha l}^C$  may now be expressed in the compact form:

$$\Gamma_{\alpha l} = m_{N_\alpha} A_{\alpha\alpha}^l(\bar{\mathbf{h}}^\nu), \quad \Gamma_{\alpha l}^C = m_{N_\alpha} A_{\alpha\alpha}^l(\bar{\mathbf{h}}^{\nu C}), \quad (4.7)$$

where we have explicitly indicated the dependence of the absorptive transition amplitudes on  $\bar{\mathbf{h}}^\nu$  and  $\bar{\mathbf{h}}^{\nu C}$ . Given the analytic expressions (4.7), it is straightforward



to compute the leptonic asymmetries for each individual lepton flavor:

$$\delta_{\alpha l} \equiv \frac{\Gamma_{\alpha l} - \Gamma_{\alpha l}^C}{\sum_{l=e,\mu,\tau} (\Gamma_{\alpha l} + \Gamma_{\alpha l}^C)} = \frac{|\bar{\mathbf{h}}_{l\alpha}^\nu|^2 - |\bar{\mathbf{h}}_{l\alpha}^{\nu C}|^2}{(\bar{\mathbf{h}}^{\nu\dagger} \mathbf{h}^\nu)_{\alpha\alpha} + (\bar{\mathbf{h}}^{\nu C\dagger} \mathbf{h}^{\nu C})_{\alpha\alpha}}. \quad (4.8)$$

The analytic results for the leptonic asymmetries  $\delta_{\alpha l}$  simplify considerably in the two-heavy neutrino-mixing limit, in which  $R_{\alpha\beta}$  defined in (4.5) is set to zero. In this limit,  $\delta_{\alpha l}$  are given by [7,8]

$$\delta_{\alpha l} \approx \frac{\text{Im}[(\mathbf{h}_{\alpha l}^{\nu\dagger} \mathbf{h}_{l\beta}^\nu)(\mathbf{h}^{\nu\dagger} \mathbf{h}^\nu)_{\alpha\beta}]}{(\mathbf{h}^{\nu\dagger} \mathbf{h}^\nu)_{\alpha\alpha} (\mathbf{h}^{\nu\dagger} \mathbf{h}^\nu)_{\beta\beta}} \times \frac{(m_{N_\alpha}^2 - m_{N_\beta}^2) m_{N_\alpha} \Gamma_{N_\beta}^{(0)}}{(m_{N_\alpha}^2 - m_{N_\beta}^2)^2 + m_{N_\alpha}^2 \Gamma_{N_\beta}^{(0)2}}, \quad (4.9)$$

where  $\alpha, \beta = 1, 2$  and  $\Gamma_{N_\alpha}^{(0)}$  is the tree-level decay width of the heavy Majorana neutrino  $N_\alpha$ , given after (4.3). Based on the simplified expression (4.9), the following two conditions for having resonantly enhanced leptonic asymmetries  $\delta_{\alpha l} \sim \mathcal{O}(1)$  may be derived [7]:

$$(i) \quad |m_{N_\alpha} - m_{N_\beta}| \sim \frac{\Gamma_{N_{\alpha,\beta}}}{2}, \quad (4.10)$$

$$(ii) \quad \frac{|\text{Im}[(\mathbf{h}_{\alpha l}^{\nu\dagger} \mathbf{h}_{l\beta}^\nu)(\mathbf{h}^{\nu\dagger} \mathbf{h}^\nu)_{\alpha\beta}]|}{(\mathbf{h}^{\nu\dagger} \mathbf{h}^\nu)_{\alpha\alpha} (\mathbf{h}^{\nu\dagger} \mathbf{h}^\nu)_{\beta\beta}} \sim 1. \quad (4.11)$$

Note that the first resonant condition (i) is exactly met, when the unitarity limit on the resummed heavy-neutrino propagator gets saturated [47], i.e. when the regulating expression in (4.9),

$$f_{\text{reg}} \equiv \frac{|m_{N_\alpha}^2 - m_{N_\beta}^2| m_{N_\alpha} \Gamma_{N_\beta}^{(0)}}{(m_{N_\alpha}^2 - m_{N_\beta}^2)^2 + m_{N_\alpha}^2 \Gamma_{N_\beta}^{(0)2}} \leq 1, \quad (4.12)$$

takes its maximal possible value:  $f_{\text{reg}} = 1$ . Within our RL scenarios, the first condition in (4.10) is naturally fulfilled as the heavy-neutrino mass splittings are generated via RG effects and are of the required order. The second condition is crucial as well and controls the size of the leptonic asymmetries. As we will see below, the condition (ii) in (4.10) has a nontrivial impact on approximate  $L$ -conserving RL models.

## B. Comparison with other methods

It is now worth commenting on some of the attempts made in the literature [48–50] to calculate the resonant part of the leptonic asymmetries  $\delta_{\alpha l}$ . Their results differ by the way in which the singularity  $m_{N_2} \rightarrow m_{N_1}$  occurring in the denominator of the second fraction in (4.9) gets regulated, when heavy-neutrino width effects are taken into consideration. Specifically, the various approaches differ in their

derivations for the analytic form of  $f_{\text{reg}}$  given in (4.12). For instance, the authors of [48] use a perturbative quantum-mechanical approach to obtain a regulator of the form:

$$f_{\text{reg}} = \frac{\Delta m_N \Gamma_{N_{1,2}}^{(0)}/2}{(\Delta m_N)^2 + \frac{1}{(16\pi)^2} m_N^2 \text{Re}^2(\mathbf{h}^{\nu\dagger} \mathbf{h}^\nu)_{12}}, \quad (4.13)$$

where  $m_N = \frac{1}{2}(m_{N_1} + m_{N_2})$  and  $\Delta m_N = |m_{N_1} - m_{N_2}|$ . It is easy to observe that for scenarios, for which  $\text{Re}(\mathbf{h}^{\nu\dagger} \mathbf{h}^\nu)_{12} = 0$ , but  $\text{Re}(\mathbf{h}_{l1}^{\nu\dagger} \mathbf{h}_{l2}^\nu) \neq 0$ , the unitarity upper bound given in (4.12) gets violated, in the degenerate heavy-neutrino mass limit  $m_{N_2} \rightarrow m_{N_1}$ . In particular, in the same limit, the individual lepton-flavor asymmetries  $\delta_{l1}$  (with  $l = e, \mu, \tau$ ) become singular. Although this singularity disappears when the lepton-flavor sum  $\delta_{N_{1,2}} = \sum_{l=e,\mu,\tau} \delta_{1,2l}$  is taken, the regulator (4.13) will still be inapplicable to lepton-flavor RL scenarios, for which  $\Delta m_N/m_N \sim \text{Re}(\mathbf{h}^{\nu\dagger} \mathbf{h}^\nu)_{12}/(16\pi) \ll \Gamma_{N_{1,2}}/m_N$ .

Based on a modified version of the field-theoretic approach introduced in [7,8], the authors of [49,50] obtain a different regulating expression for the leptonic asymmetry  $\delta_{1l}$ :

$$f_{\text{reg}} = \frac{|m_{N_1}^2 - m_{N_2}^2| m_{N_1} \Gamma_{N_2}^{(0)}}{(m_{N_1}^2 - m_{N_2}^2)^2 + (m_{N_1} \Gamma_{N_1}^{(0)} - m_{N_2} \Gamma_{N_2}^{(0)})^2}. \quad (4.14)$$

It is not difficult to observe that  $f_{\text{reg}}$  diverges as  $(m_{N_1} - m_{N_2})^{-1}$  in RL scenarios, for which  $(\mathbf{h}^{\nu\dagger} \mathbf{h}^\nu)_{11} = (\mathbf{h}^{\nu\dagger} \mathbf{h}^\nu)_{22}$ , even though one could still have  $(\mathbf{h}_{l1}^{\nu\dagger} \mathbf{h}_{l1}^\nu) \neq (\mathbf{h}_{l2}^{\nu\dagger} \mathbf{h}_{l2}^\nu)$  for each single lepton flavor  $l$ . For instance, such a situation can naturally occur in approximate lepton-number conserving models of RL discussed recently in [51,52]. Evidently, the prediction for the leptonic asymmetries  $\delta_{N_{1,2}}$  in such scenarios may get overestimated by many orders of magnitude.

In order to illustrate this last point, let us consider a one-generation inverse seesaw model [53] with two singlet neutrinos of opposite lepton number,  $\nu_R$  and  $S_L$ . The neutrino sector of this model is described by the lepton-number-conserving Lagrangian

$$-\mathcal{L}_{\text{inverse}} = \frac{1}{2} (\bar{S}_L, \bar{\nu}_R^C) \begin{pmatrix} 0 & M \\ M & 0 \end{pmatrix} \begin{pmatrix} S_L^C \\ \nu_R \end{pmatrix} + h_R (\bar{\nu}_L, \bar{l}_L) \tilde{\Phi} \nu_R + \text{H.c.} \quad (4.15)$$

Without loss of generality, the kinematic parameters  $M$  and  $h_R$  can be rephased to become real. Following closely the discussion in [7], we introduce into the Lagrangian (4.15) the lepton-number violating operators  $\frac{1}{2} \mu_R \bar{\nu}_R^C \nu_R$ ,  $\frac{1}{2} \mu_L \bar{S}_L^C S_L$  and  $h_L (\bar{\nu}_L, \bar{l}_L) \tilde{\Phi} S_L^C$ . In order to minimally break both the lepton number and  $CP$ , it was shown in [7] that at least two of the aforementioned  $\Delta L = 2$  operators are needed. In fact, this result is a direct consequence of the Nanopoulos–Weinberg (NW) no-go theorem [54].

The NW theorem states that no net baryon asymmetry can be generated by a single  $B$ - and  $CP$ -violating operator to all orders in perturbation theory.

It is interesting to provide an estimate of the lepton asymmetry obtained within a simple model of approximate lepton-number conservation, where  $\mu_L = -i\mu_R = \mu$  and  $h_L = 0$ . For these parameters, we adopt the same ballpark of values as in [51]:  $m_N \approx M = 1$  TeV,  $h_R = 3 \times 10^{-2}$  and  $\Delta m_N \approx \mu/\sqrt{2} = 2 \times 10^{-10}M$ . With these input parameters, we may estimate that  $\Gamma_{N_{1,2}}^{(0)} \approx 2 \times 10^{-5}m_N$ , leading to  $\Delta m_N/\Gamma_{N_{1,2}}^{(0)} \approx 10^{-5}$ . The first fraction containing the  $CP$ -violating phases in (4.9) is rather suppressed, of order  $\mu/M \sim \Delta m_N/m_N \sim 10^{-10}$ , while  $f_{\text{reg}} \approx 2\Delta m_N/\Gamma_{N_{1,2}} \approx 2 \times 10^{-5}$  within our resummation approach. This gives rise to dismally small lepton asymmetries:

$$\delta_{1l} \approx \delta_{2l} \sim \frac{\mu}{M} \frac{\mu}{\Gamma_{N_{1,2}}} \sim 10^{-15}. \quad (4.16)$$

Notice that the lepton asymmetries  $\delta_{1,2l}$  are proportional to  $\mu^2$  in agreement with the NW theorem and, as they should, both vanish identically in the  $L$ -conserving limit  $\mu \rightarrow 0$ . As we will see in the next section, lepton asymmetries of order  $10^{-15}$  will fall short by at least 7 orders of magnitude to explain the BAU. Instead, had one used the regulator  $f_{\text{reg}}$  in (4.14), one would have obtained the enormous enhancement:  $f_{\text{reg}} \approx \Gamma_{N_{1,2}}/\mu \sim 10^5 \gg 1$ , leading to lepton asymmetries of order [51]:  $\delta_{1,2l} \sim \Gamma_{N_{1,2}}/m_N \sim 10^{-5}$ . However, this result is independent of the  $L$ -conserving parameter  $\mu = \mu_L = -i\mu_R$ , and taking the  $L$ -conserving limit  $\mu \rightarrow 0$ , one obtains a nonzero lepton asymmetry, which clearly signifies an erroneous result. The above exercise shows that one has to go beyond the two-heavy neutrino-mixing framework and consider nontrivial lepton-flavor effects [13], in order to obtain a phenomenologically relevant model that predicts testable rates for LFV.

### C. Baryon asymmetry

In this section we present the relevant Boltzmann equations (BEs) which will be used to evaluate the heavy-Majorana-neutrino-, the lepton- and the baryon-number densities,  $\eta_{N_{1,2,3}} = n_{N_{1,2,3}}/n_\gamma$ ,  $\eta_{L_{e,\mu,\tau}} = n_{L_{e,\mu,\tau}}/n_\gamma$  and  $\eta_B = n_B/n_\gamma$ , normalized to the photon number density  $n_\gamma$ . In our computations, we include the dominant collision terms related to the  $1 \rightarrow 2$  decays of the right-handed neutrinos and to resonant  $2 \rightarrow 2$  lepton scatterings that describe  $\Delta L = 2$  and  $\Delta L = 0$  transitions. We neglect chemical potential contributions from the right-handed charged leptons and quarks.

In order to appropriately take into account the flavor effects on the BEs for  $\eta_{N_{1,2,3}}$  and  $\eta_{L_{e,\mu,\tau}}$ , we closely follow the approach and the notation established in [14]. More explicitly, the BEs are found to be

$$\frac{d\eta_{N_\alpha}}{dz} = -\frac{z}{n_\gamma H_N} \left( \frac{\eta_{N_\alpha}^{\text{eq}}}{\eta_N^{\text{eq}}} - 1 \right) \gamma_{L\Phi}^{N_\alpha}, \quad (4.17)$$

$$\begin{aligned} \frac{d\eta_{L_l}}{dz} = & \frac{z}{n_\gamma H_N} \left[ \sum_{\alpha=1}^3 \left( \frac{\eta_{N_\alpha}^{\text{eq}}}{\eta_N^{\text{eq}}} - 1 \right) \delta_{\alpha l} \gamma_{L\Phi}^{N_\alpha} \right. \\ & - \frac{2}{3} \eta_{L_l} \sum_{k=e,\mu,\tau} (\gamma_{L_k^c \Phi^\dagger}^{L_l \Phi} + \gamma_{L_k \Phi}^{L_l \Phi}) \\ & \left. - \frac{2}{3} \sum_{k=e,\mu,\tau} \eta_{L_k} (\gamma_{L_l^c \Phi^\dagger}^{L_k \Phi} - \gamma_{L_l \Phi}^{L_k \Phi}) \right], \quad (4.18) \end{aligned}$$

where  $\alpha = 1, 2, 3$  and  $l = e, \mu, \tau$ . In addition,  $H_N \approx 17 \times m_N^2/M_P$  is the Hubble parameter at  $T = m_N$ , where  $M_P = 1.2 \times 10^{19}$  GeV is the Planck mass. The  $T$ -dependence of the BEs (4.17) and (4.18) is expressed by virtue of the dimensionless parameter

$$z = \frac{m_N}{T}, \quad (4.19)$$

in terms of which the photon number density is given by

$$n_\gamma = \frac{2T^3}{\pi^2} \zeta(3) = \frac{2m_N^3}{\pi^2} \frac{\zeta(3)}{z^3}, \quad (4.20)$$

where  $\zeta(3) \approx 1.202$  is Apéry's constant. Finally,  $\eta_N^{\text{eq}}$  in (4.17) and (4.18) is the equilibrium number density of the heavy Majorana neutrino  $N_\alpha$ , normalized to the number density of photons, i.e.

$$\eta_N^{\text{eq}} \approx \frac{1}{2} z^2 K_2(z), \quad (4.21)$$

where  $K_n(x)$  is the  $n$ th-order modified Bessel function [55].

The BEs (4.17) and (4.18) include the collision terms for the decays  $N_\alpha \rightarrow L_l \Phi$ , as well as the  $\Delta L = 0$ , two resonant scatterings:  $L_k \Phi \leftrightarrow L_l \Phi$  and  $L_k \Phi \leftrightarrow L_l^c \Phi^\dagger$ , which are defined as [14]

$$\begin{aligned} \gamma_{L\Phi}^{N_\alpha} & \equiv \sum_{k=e,\mu,\tau} [\gamma(N_\alpha \rightarrow L_k \Phi) + \gamma(N_\alpha \rightarrow L_k^c \Phi^\dagger)], \\ \gamma_{L_l \Phi}^{L_k \Phi} & \equiv \gamma(L_k \Phi \rightarrow L_l \Phi) + \gamma(L_k^c \Phi^\dagger \rightarrow L_l^c \Phi^\dagger), \\ \gamma_{L_l^c \Phi^\dagger}^{L_k \Phi} & \equiv \gamma(L_k \Phi \rightarrow L_l^c \Phi^\dagger) + \gamma(L_k^c \Phi^\dagger \rightarrow L_l \Phi). \end{aligned} \quad (4.22)$$

Since we are only interested in the resonant part of the above  $2 \rightarrow 2$  scatterings, we make use of the narrow width approximation (NWA) for the resummed heavy-neutrino propagators. Thus, at the amplitude squared level, we employ the NWA for the complex-conjugate product of Breit-Wigner propagators [56]:

$$\begin{aligned} & \frac{1}{s - m_{N_\alpha}^2 - im_{N_\alpha} \Gamma_{N_\alpha}} \frac{1}{s - m_{N_\beta}^2 + im_{N_\beta} \Gamma_{N_\beta}} \\ & \approx \frac{i\pi [\delta(s - m_{N_\alpha}^2) + \delta(s - m_{N_\beta}^2)]}{m_{N_\alpha}^2 - m_{N_\beta}^2 + \frac{i}{2}(m_{N_\alpha} + m_{N_\beta})(\Gamma_{N_\alpha} + \Gamma_{N_\beta})}. \end{aligned} \quad (4.23)$$

Note that the NWA relation (4.23) is valid for any range of parameter values for  $\Gamma_{N_{1,2,3}}$  and  $m_{N_{1,2,3}}$ , as long as  $\Gamma_{N_{1,2,3}} \ll m_{N_{1,2,3}}$ . This last condition is naturally fulfilled within the  $R\ell L$  models.

The collision term pertinent to the heavy-Majorana-neutrino decays  $\gamma_{L\Phi}^{N_\alpha}$  is given by

$$\gamma_{L_i\Phi}^{L_k} = \sum_{\alpha,\beta=1}^3 (\gamma_{L\Phi}^{N_\alpha} + \gamma_{L\Phi}^{N_\beta}) \frac{2(\bar{\mathbf{h}}_{l\alpha}^{\nu*} \bar{\mathbf{h}}_{k\alpha}^{\nu C*} \bar{\mathbf{h}}_{l\beta}^{\nu} \bar{\mathbf{h}}_{k\beta}^{\nu C} + \bar{\mathbf{h}}_{l\alpha}^{\nu C*} \bar{\mathbf{h}}_{k\alpha}^{\nu*} \bar{\mathbf{h}}_{l\beta}^{\nu C} \bar{\mathbf{h}}_{k\beta}^{\nu})}{[(\bar{\mathbf{h}}^{\nu\dagger} \bar{\mathbf{h}}^\nu)_{\alpha\alpha} + (\bar{\mathbf{h}}^{\nu C\dagger} \bar{\mathbf{h}}^{\nu C})_{\alpha\alpha} + (\bar{\mathbf{h}}^{\nu\dagger} \bar{\mathbf{h}}^\nu)_{\beta\beta} + (\bar{\mathbf{h}}^{\nu C\dagger} \bar{\mathbf{h}}^{\nu C})_{\beta\beta}]^2} \left(1 - 2i \frac{m_{N_\alpha} - m_{N_\beta}}{\Gamma_{N_\alpha} + \Gamma_{N_\beta}}\right)^{-1}, \quad (4.25)$$

$$\gamma_{L_i^c\Phi^\dagger}^{L_k} = \sum_{\alpha,\beta=1}^3 (\gamma_{L\Phi}^{N_\alpha} + \gamma_{L\Phi}^{N_\beta}) \frac{2(\bar{\mathbf{h}}_{l\alpha}^{\nu*} \bar{\mathbf{h}}_{k\alpha}^{\nu*} \bar{\mathbf{h}}_{l\beta}^{\nu} \bar{\mathbf{h}}_{k\beta}^{\nu} + \bar{\mathbf{h}}_{l\alpha}^{\nu C*} \bar{\mathbf{h}}_{k\alpha}^{\nu C*} \bar{\mathbf{h}}_{l\beta}^{\nu C} \bar{\mathbf{h}}_{k\beta}^{\nu C})}{[(\bar{\mathbf{h}}^{\nu\dagger} \bar{\mathbf{h}}^\nu)_{\alpha\alpha} + (\bar{\mathbf{h}}^{\nu C\dagger} \bar{\mathbf{h}}^{\nu C})_{\alpha\alpha} + (\bar{\mathbf{h}}^{\nu\dagger} \bar{\mathbf{h}}^\nu)_{\beta\beta} + (\bar{\mathbf{h}}^{\nu C\dagger} \bar{\mathbf{h}}^{\nu C})_{\beta\beta}]^2} \left(1 - 2i \frac{m_{N_\alpha} - m_{N_\beta}}{\Gamma_{N_\alpha} + \Gamma_{N_\beta}}\right)^{-1}. \quad (4.26)$$

The scattering collision terms (4.25) and (4.26) contain all contributions from the resonant exchange of right-handed neutrinos in the NWA, including contributions from the so-called real intermediate states (RISs) [57]. The latter are obtained when only the diagonal terms  $\alpha = \beta$  are taken in the summation over the heavy Majorana states  $N_{\alpha,\beta}$ .

Separating the diagonal  $\alpha = \beta$  RIS contributions from the off-diagonal  $\alpha \neq \beta$  terms in the sum, we may rewrite the BE (4.18) in the form [14]

$$\begin{aligned} \frac{d\eta_{L_i}}{dz} = & \frac{z}{n_\gamma H_N} \left\{ \sum_{\alpha=1}^3 \left( \frac{\eta_{N_\alpha}}{\eta_N^{\text{eq}}} - 1 \right) \delta_{\alpha i} \gamma_{L\Phi}^{N_\alpha} \right. \\ & - \frac{2}{3} \eta_{L_i} \left[ \sum_{\alpha=1}^3 \gamma_{L\Phi}^{N_\alpha} B_{\alpha i} + \sum_{k=e,\mu,\tau} (\gamma_{L_k^c\Phi^\dagger}^{L_i} + \gamma_{L_k\Phi}^{L_i}) \right] \\ & \left. - \frac{2}{3} \sum_{k=e,\mu,\tau} \eta_{L_k} \left[ \sum_{\alpha=1}^3 \delta_{\alpha i} \delta_{\alpha k} \gamma_{L\Phi}^{N_\alpha} + (\gamma_{L_i^c\Phi^\dagger}^{L_k} - \gamma_{L_i\Phi}^{L_k}) \right] \right\}, \end{aligned} \quad (4.27)$$

where  $\gamma_Y^{X} = \gamma_Y^X - (\gamma_Y^X)_{\text{RIS}}$  denote the RIS-subtracted collision terms and  $B_{\alpha i}$  are the branching ratios

$$B_{\alpha i} = \frac{\Gamma_{\alpha i} + \Gamma_{\alpha i}^C}{\sum_{k=e,\mu,\tau} (\Gamma_{\alpha k} + \Gamma_{\alpha k}^C)} = \frac{|\bar{\mathbf{h}}_{i\alpha}^\nu|^2 + |\bar{\mathbf{h}}_{i\alpha}^{\nu C}|^2}{(\bar{\mathbf{h}}^{\nu\dagger} \bar{\mathbf{h}}^\nu)_{\alpha\alpha} + (\bar{\mathbf{h}}^{\nu C\dagger} \bar{\mathbf{h}}^{\nu C})_{\alpha\alpha}}. \quad (4.28)$$

The collision terms proportional to  $\eta_{L_k}$  and to  $\delta_{\alpha i} \delta_{\alpha k}$  on the right-hand side of (4.27) turn out to be numerically negligible for the  $R\ell L$  scenarios under consideration. Instead, the RIS-subtracted collision terms proportional to  $\eta_{L_i}$  in (4.27) become significant. Their importance in RL models was originally raised in [8,14] and confirmed most recently in [51].

The next step is to include the effect of the  $(B + L)$ -violating sphaleron processes [6]. For temperatures  $T$  larger than the critical temperature  $T_c \approx 135$  GeV

$$\gamma_{L\Phi}^{N_\alpha} = \frac{m_N^3}{\pi^2 z} K_1(z) \Gamma_{N_\alpha}, \quad (4.24)$$

while the corresponding collision terms for the  $\Delta L = 0$ , 2 lepton-flavor transitions are calculated by means of the NWA (4.23) to be

of the electroweak phase transition, the conversion of the total lepton-to-photon ratio  $\sum_{l=e,\mu,\tau} \eta_{L_l}$  to the baryon-to-photon ratio  $\eta_B^c$  at  $T_c$  is given by the relation:

$$\eta_B^c = -\frac{28}{51} \sum_{l=e,\mu,\tau} \eta_{L_l}. \quad (4.29)$$

For  $T < T_c$ , the so-generated baryon asymmetry  $\eta_B^c$  gets diluted by standard photon interactions until the recombination epoch, leading to the BAU

$$\eta_B \approx \frac{1}{27} \eta_B^c. \quad (4.30)$$

This theoretical prediction can now be compared with the current observational value for the baryon-to-photon asymmetry [2],

$$\eta_B^{\text{obs}} = (6.20 \pm 0.15) \times 10^{-10}. \quad (4.31)$$

It is instructive to derive approximate numerical solutions to the BEs (4.17) and (4.27). To this end, we reexpress the BEs in terms of the out-of-equilibrium deviation parameters  $\delta\eta_{N_\alpha} = \eta_{N_\alpha}/\eta_N^{\text{eq}} - 1$  and neglect the suppressed  $\mathcal{O}(\delta_{\alpha i}^2)$  collision terms. For simplicity, we initially ignore the RIS-subtracted collision terms. But, as we will see below, their inclusion is straightforward. With these approximations and simplifications, the BEs may be recast into the compact form:

$$\frac{d\delta\eta_{N_\alpha}}{dz} = \frac{K_1(z)}{K_2(z)} [1 + (1 - K_\alpha z) \delta\eta_{N_\alpha}], \quad (4.32)$$

$$\frac{d\eta_{L_i}}{dz} = z^3 K_1(z) \sum_{\alpha=1}^3 K_\alpha (\delta\eta_{N_\alpha} \delta_{\alpha i} - \frac{2}{3} B_{\alpha i} \eta_{L_i}), \quad (4.33)$$

with  $K_\alpha = \Gamma_{N_\alpha}/[\zeta(3)H_N]$ . In the kinematic regime  $z > z_1^\alpha \approx 2K_\alpha^{-1/3}$ , the solution to (4.32) may well be approximated by

$$\delta\eta_{N_\alpha}(z) = (K_\alpha z)^{-1}, \quad (4.34)$$

independently of the initial conditions (see Fig. 1). In this regime, the BE (4.33) becomes

$$\frac{d\eta_{L_l}}{dz} = z^2 K_1(z) \left( \delta_l - \frac{2}{3} z K_l \eta_{L_l} \right), \quad (4.35)$$

$$\begin{aligned} \kappa_l &\equiv \frac{\sum_{k=e,\mu,\tau} (\gamma_{L_k^c \Phi^\dagger}^{L_l \Phi} + \gamma_{L_k \Phi}^{L_l \Phi}) + \gamma_{L_l^c \Phi^\dagger}^{L_l \Phi} - \gamma_{L_l \Phi}^{L_l \Phi}}{\sum_{\alpha=1}^3 \gamma_{L \Phi}^{N_\alpha} B_{\alpha l}} \\ &= 2 \sum_{\alpha,\beta=1}^3 \frac{(\bar{\mathbf{h}}_{\alpha l}^{\nu\dagger} \bar{\mathbf{h}}_{l\beta}^\nu + \bar{\mathbf{h}}_{\alpha l}^{\nu C\dagger} \bar{\mathbf{h}}_{l\beta}^{\nu C}) [(\bar{\mathbf{h}}^{\nu\dagger} \bar{\mathbf{h}}^\nu)_{\alpha\beta} + (\bar{\mathbf{h}}^{\nu C\dagger} \bar{\mathbf{h}}^{\nu C})_{\alpha\beta}] + (\bar{\mathbf{h}}_{\alpha l}^{\nu\dagger} \bar{\mathbf{h}}_{l\beta}^\nu - \bar{\mathbf{h}}_{\alpha l}^{\nu C\dagger} \bar{\mathbf{h}}_{l\beta}^{\nu C})^2}{[(\bar{\mathbf{h}}^\nu \bar{\mathbf{h}}^{\nu\dagger})_{ll} + (\bar{\mathbf{h}}^{\nu C} \bar{\mathbf{h}}^{\nu C\dagger})_{ll}] [(\bar{\mathbf{h}}^{\nu\dagger} \bar{\mathbf{h}}^\nu)_{\alpha\alpha} + (\bar{\mathbf{h}}^{\nu C\dagger} \bar{\mathbf{h}}^{\nu C})_{\alpha\alpha} + (\bar{\mathbf{h}}^{\nu\dagger} \bar{\mathbf{h}}^\nu)_{\beta\beta} + (\bar{\mathbf{h}}^{\nu C\dagger} \bar{\mathbf{h}}^{\nu C})_{\beta\beta}]} \\ &\quad \times \left( 1 - 2i \frac{m_{N_\alpha} - m_{N_\beta}}{\Gamma_{N_\alpha} + \Gamma_{N_\beta}} \right)^{-1}. \end{aligned} \quad (4.36)$$

In determining the scaling factor  $\kappa_l$ , we have assumed that  $\eta_{L_l} \gg \eta_{L_{k \neq l}}$  in (4.18), which is a valid approximation within a given R $\ell$ L scenario under study. Note that if only the diagonal  $\alpha = \beta$  terms representing the RIS contributions are considered in the sum,  $\kappa_l$  reaches its maximum value, i.e.  $\kappa_l = 1 + \mathcal{O}(\delta_l^2)$ . We also have checked that in the  $L_l$ -conserving limit of the theory, the parameter  $\kappa_l$  vanishes, as it should.

As is illustrated in Fig. 1, the solution  $\eta_{L_l}$  to (4.35) exhibits different behavior in the three kinematic regimes, characterized by the specific values of the parameter  $z = m_N/T$ :

$$z_2^l \approx 2(K_l^{\text{eff}})^{-1/3}, \quad z_3^l \approx 1.25 \ln(25K_l^{\text{eff}}). \quad (4.37)$$

For  $z$  values in the range  $z_2^l < z < z_3^l$ , the solution  $\eta_{L_l}$  may well be approximated by

$$\eta_{L_l}(z) = \frac{3}{2} \frac{\delta_l}{K_l^{\text{eff}} z}. \quad (4.38)$$

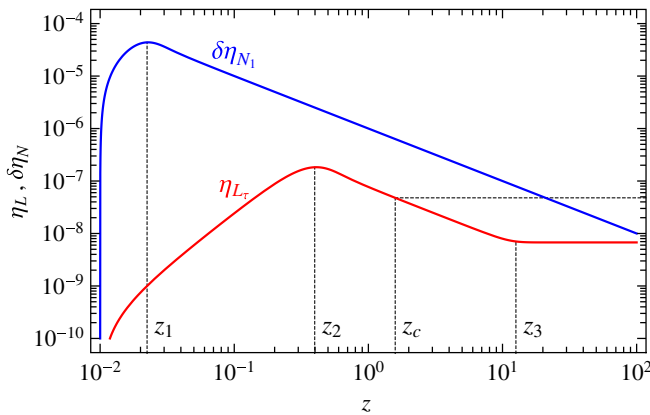


FIG. 1 (color online). Numerical solutions to BEs (4.32) and (4.35) for  $\delta\eta_{N_1} = \eta_{N_1}/\eta_{N_1}^{\text{eq}} - 1$  and  $\eta_{L_\tau}$ , respectively, in a R $\tau$ L model with  $m_N = 220$  GeV,  $K_1 = 10^6$ ,  $K_\tau^{\text{eff}} = 10^2$ ,  $\delta_\tau = 10^{-6}$  and  $z_c = m_N/T_c = 1.6$ .

with  $\delta_l = \sum_{\alpha=1}^3 \delta_{\alpha l}$  and  $K_l = \sum_{\alpha=1}^3 K_\alpha B_{\alpha l}$ . We may include the numerically significant RIS-subtracted collision terms proportional to  $\eta_{L_l}$  in (4.27), by rescaling  $K_l \rightarrow \kappa_l K_l \equiv K_l^{\text{eff}}$ , where

For  $z > z_3^l$ , the lepton-number density  $\eta_{L_l}$  freezes out and approaches the constant value  $\eta_{L_l} = (3\delta_l)/(2K_l^{\text{eff}} z_3^l)$ .<sup>2</sup> The general behavior of  $\eta_{L_l}$  in the different regimes is displayed in Fig. 1.

In this paper we only consider R $\ell$ L scenarios, for which the washout is strong enough, such that the critical temperature  $z_c = m_N/T_c$  where the baryon asymmetry  $\eta_B$  decouples from the lepton asymmetries  $\eta_{L_l}$  is situated in the linear dropoff or constant regime. Specifically, we require that

$$z_c > 2K_\alpha^{-1/3}, \quad z_c > 2(K_l^{\text{eff}})^{-1/3}, \quad (4.39)$$

for all heavy-neutrino species  $N_\alpha = N_{1,2,3}$  and lepton flavors  $l = e, \mu, \tau$ . As a consequence, the baryon asymmetry  $\eta_B$  becomes relatively independent of the initial values of  $\eta_{L_l}$  and  $\eta_{N_\alpha}$ . In this case, taking into account all factors in (4.29), (4.30), and (4.38), the resulting BAU is estimated to be

$$\begin{aligned} \eta_B &= -\frac{28}{51} \frac{1}{27} \frac{3}{2} \sum_{l=e,\mu,\tau} \frac{\delta_l}{K_l^{\text{eff}} \min(z_c, z_3^l)} \\ &\approx -3 \cdot 10^{-2} \sum_{l=e,\mu,\tau} \frac{\delta_l}{K_l^{\text{eff}} \min[m_N/T_c, 1.25 \ln(25K_l^{\text{eff}})]}. \end{aligned} \quad (4.40)$$

We note that the formula (4.40) provides a fairly good estimate of the BAU  $\eta_B$  to less than 20%, in the applicable regime of approximations given by (4.39) for  $K_l^{\text{eff}} \geq 5$  for a right-handed neutrino mass scale of the order of the electroweak scale. Hence, to account for the observed BAU  $\eta_B^{\text{obs}}$  given in (4.31), lepton asymmetries  $\delta_l \geq 10^{-7}$  are required. In the next section, we present numerical estimates of the

<sup>2</sup>The onset of the freeze-out is defined as the position  $z_3^l$  where the relative slope of (4.35) drops below 1, i.e. when  $|\eta'_{L_l}/\eta_{L_l}| = 2/3(z_3^l)^3 K_1(z_3^l) K_l^{\text{eff}} = 1$ . The solution to this equation can be analytically expressed in terms of the Lambert  $W$  function, to which  $z_3^l$  in (4.37) proves to be an excellent interpolating approximation over the wide range of values  $K_l^{\text{eff}} \approx 2 - 10^{10}$ .



BAU for R $\ell$ L scenarios, based on the simplified BEs (4.32) and (4.35), with  $K_l$  replaced by  $K_l^{\text{eff}}$  as defined by means of (4.36).

## V. NUMERICAL RESULTS

In this section we present numerical estimates of the BAU  $\eta_B$  and the low-energy LFV observables for  $\mu \rightarrow e$  and  $\tau \rightarrow (e, \mu)$  transitions, based on the analytic results derived in Secs. III and IV. Our aim is to delineate the viable parameter space of the R $\ell$ L models: R $\tau$ L, R $\mu$ L and ReL, by considering both cases of a normal and inverted hierarchy for the light-neutrino mass spectrum. In all the R $\ell$ L scenarios under study, the lightest neutrino is massless. As described in Sec. II, we use the neutrino oscillation data to determine the theoretical parameters of the light-neutrino mass matrix  $\mathbf{m}^\nu$ . Specifically, we invert the seesaw formula and solve for the neutrino Yukawa couplings  $a$ ,  $b$  and  $\epsilon_{e,\mu,\tau}$ . In addition, the electroweak-scale flavor structure of the right-handed neutrino mass matrix  $\mathbf{m}_M$  is generated from a flavor-universal heavy-neutrino mass matrix  $\mathbf{m}_M(M_X) = m_N \mathbf{1}_3$  at the GUT scale  $M_X$ , after taking into account RG-running effects.

For a given light-neutrino mass matrix  $\mathbf{m}^\nu$ , the solution obtained for  $a$  and  $b$  is unique up to a common sign factor. This sign degeneracy could be eliminated, only if the sign of  $\text{Re}(a)$  were known. There is also a similar freedom for an overall sign in the  $\epsilon_{e,\mu,\tau}$  parameters, but this turns out to be irrelevant, since it applies to a complete column in the neutrino Yukawa matrix  $\mathbf{h}^\nu$  and can be rotated away. In addition to the light-neutrino masses and mixings, the light-neutrino mass matrix may also contain the  $CP$ -violating Dirac phase  $\delta$  and the Majorana phases  $\phi_{1,2}$ . As our ansatz for the neutrino Yukawa matrix  $\mathbf{h}^\nu$  uses maximal  $CP$  phases for  $a$  and  $b$ , the inclusion of the light-neutrino  $CP$  phases is not expected to increase or change significantly our predictions for the baryon asymmetry  $\eta_B$ . We therefore consider only the extreme cases of  $CP$  parities,  $\delta$ ,  $\phi_{1,2} = 0, \pi$ , as natural choices which can help us to reduce the dimensionality of the parameter space. As well as  $\sin^2\theta_{12}$ ,  $\sin^2\theta_{23}$ ,  $\sin^2\theta_{13}$ ,  $\Delta m_{12}^2$ ,  $|\Delta m_{13}^2|$ , the sign of  $(\Delta m_{13}^2)$ ,  $\delta$  and  $\phi_{1,2}$ , we also have the free parameters  $\kappa_{1,2}$ ,  $\gamma_{1,2}$ , the sign of  $\text{Re}(a)$  and  $m_N$  in our R $\ell$ L models. Unless otherwise stated, we use the best fit values of [27] for the measured neutrino oscillation parameters.

To start with, we show in Fig. 2 numerical estimates of the baryon asymmetry  $\eta_B$  and the LFV observables  $B(\mu \rightarrow e\gamma)$  and  $B_{\mu e}(^{48}\text{Ti})$ , as functions of the Yukawa-coupling parameters  $\kappa_1$  and  $\kappa_2$ , in a R $\tau$ L model with  $m_N = 120$  GeV and a normal hierarchical light-neutrino mass spectrum. The neutrino-mixing angle  $\sin^2\theta_{13}$  is set to its upper experimental  $2\sigma$  limit [27]:  $\sin^2\theta_{13} = 0.033$ . The remaining theoretical parameters are chosen to maximise the overlap between successful generation of the required baryon asymmetry and high LFV rates.

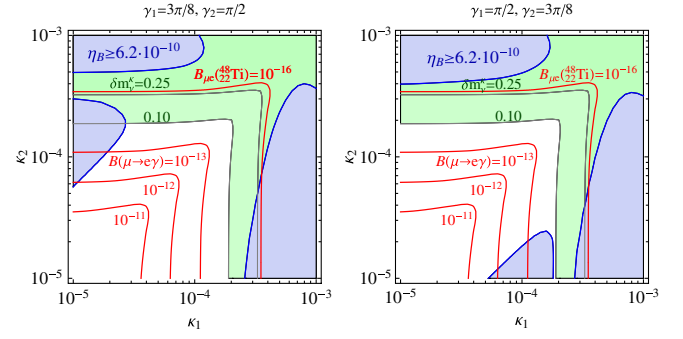


FIG. 2 (color online). The baryon asymmetry  $\eta_B$  and the LFV observables  $B(\mu \rightarrow e\gamma)$  and  $B_{\mu e}(^{48}\text{Ti})$  as functions of  $\kappa_1$  and  $\kappa_2$  in the R $\tau$ L model with  $m_N = 120$  GeV, assuming a normal light-neutrino mass spectrum. The remaining parameters were chosen to be:  $\gamma_1 = 3\pi/8$ ,  $\gamma_2 = \pi/2$ ,  $\phi_1 = \pi$ ,  $\phi_2 = 0$ ,  $\text{Re}(a) > 0$  (left panel);  $\gamma_1 = \pi/2$ ,  $\gamma_2 = 3\pi/8$ ,  $\phi_1 = 0$ ,  $\phi_2 = 0$ ,  $\text{Re}(a) < 0$  (right panel). The neutrino oscillation parameters are set at their best fit values, with  $\sin^2\theta_{13} = 0.033$  at its  $2\sigma$  upper limit. The dark (blue) shaded regions denote the parameter space where the baryon asymmetry is larger than the observational value  $\eta_B^{\text{obs}} = 6.2 \times 10^{-10}$ . The light (green) shaded areas labeled as ‘ $\delta m_\nu^\kappa = 0.25$ ’ and ‘0.10’ indicate the parameter space where the inversion of the light-neutrino mass matrix is violated at the 25% and 10% level, respectively.

For definiteness, we set  $\gamma_1 = 3\pi/8$ ,  $\gamma_2 = 1/2\pi$  (left panel) and  $\gamma_1 = 1/2\pi$ ,  $\gamma_2 = 3\pi/8$  (right panel). The blue shaded areas denote the parameter space where the numerically predicted baryon asymmetry  $\eta_B$  is larger than the observational value  $\eta_B^{\text{obs}} = 6.2 \times 10^{-10}$ . These areas should be regarded as representing regions of viable parameter space for successful leptogenesis, given the freedom of readjusting the  $CP$  phases  $\gamma_{1,2}$  of the Yukawa couplings  $\kappa_{1,2}$ .

The parameters  $\kappa_{1,2}$  are varied within the range  $10^{-5} - 10^{-3}$ ; smaller values of  $\kappa_{1,2}$  would lead to too large values for  $a$ ,  $b > 0.1$ , whereas larger  $\kappa_{1,2}$  values would violate the assumed approximation  $\kappa_{1,2} \ll a, b$ , required to invert the seesaw formula. The degree of violation of this approximation is indicated by the light (green) shaded areas in Fig. 2. These areas denote the parameter space, in which the quantity

$$\delta m_\nu^\kappa \equiv \frac{\Delta m_N}{m_N} \left( \frac{\max(\kappa_1, \kappa_2)}{\min(|\epsilon_e|, |\epsilon_\mu|, |\epsilon_\tau|)} \right)^2 \quad (5.1)$$

is bigger than 0.25 and 0.10, respectively. The quantity  $\delta m_\nu^\kappa$  is a measure that quantifies the accuracy of our analytic approximation for neglecting the contribution of the neutrino Yukawa couplings  $\kappa_{1,2}$  in the light-neutrino mass matrix  $\mathbf{m}^\nu$  [cf. (2.13)]. Hence, the values of  $\delta m_\nu^\kappa = 0.10$  and  $0.25$  mean that the inversion of the light-neutrino mass matrix is accurate at the 10% and 25% level, respectively, due to the assumed absence of the  $\kappa_{1,2}$  terms.

It should be stressed that the corresponding parameter space is not ruled out; larger values of  $\kappa_{1,2} \gtrsim 5 \times 10^{-4}$  would require a numerical approach to invert the light-neutrino mass matrix  $\mathbf{m}^\nu$ , beyond our analytic approximation.

The specific choice for the phases  $\gamma_{1,2}$  in Fig. 2 approximately maximises the numerically predicted baryon asymmetry  $\eta_B$  compatible with testable LFV decay rates. Specifically, the areas around  $(\kappa_1, \kappa_2) \approx (10^{-5}, 10^{-4})$  (left panel) and  $(10^{-4}, 10^{-5})$  (right panel), where  $B(\mu \rightarrow e\gamma) \approx 10^{-12}$  can be achieved, are only present for sufficiently asymmetric values  $\gamma_1 \neq \gamma_2$ , and only for specific choices for the remaining discrete parameters in the R $\tau$ L model. As a consequence, the requirement of both a successful generation of the baryon asymmetry  $\eta_B$  and potentially observable LFV rates for  $\mu \rightarrow e$  transitions puts severe constraints on the model parameter space. We note that the dependence of the baryon asymmetry  $\eta_B$  on the right-handed neutrinos mass scale  $m_N$  is weak in the physically interesting region of  $m_N = 100\text{--}500$  GeV. Finally, the LFV  $\tau$  decays are extremely suppressed with  $B(\tau \rightarrow l_2\gamma) \sim 10^{-17}$  ( $l_2 = e, \mu$ ), and so remain far beyond the realm of detection.

In Fig. 3 we display numerical estimates of  $\eta_B$  and the LFV observables  $B(\mu \rightarrow e\gamma)$  and  $B_{\mu e}(\frac{48}{22}\text{Ti})$ , as functions of  $\kappa_1$  and  $\kappa_2$ , in a R $\tau$ L model with  $m_N = 120$  GeV and an inverted hierarchical light-neutrino mass spectrum, characterized by  $\Delta m_{13}^2 < 0$ . As before, we set the neutrino-mixing angle  $\sin^2\theta_{13}$  to its upper experimental  $2\sigma$  limit [27]:  $\sin^2\theta_{13} = 0.033$ . As can be seen from Fig. 3, the regions of the parameter space that yield successful baryon asymmetry  $\eta_B$  are smaller than those found in the normal hierarchical case for the light-neutrino mass spectrum. If such a scenario gets realized in nature, then successful leptogenesis implies rates for  $B_{\mu e}(\frac{48}{22}\text{Ti}) \lesssim 10^{-16}$ , which can still be within reach of the projected PRISM experiment [21].

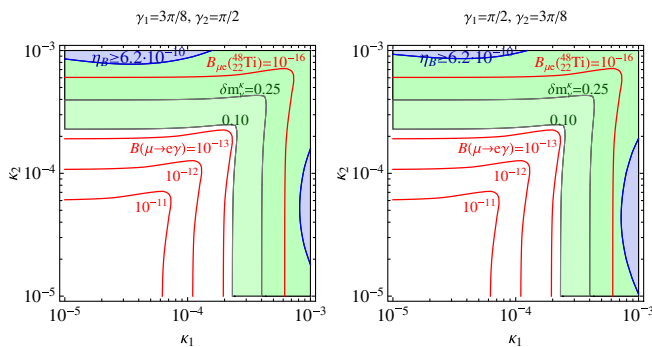


FIG. 3 (color online). The same as in Fig. 2, but assuming an inverted light-neutrino mass spectrum. The remaining parameters were chosen as follows:  $\gamma_1 = 3\pi/8$ ,  $\gamma_2 = \pi/2$ ,  $\phi_1 = \pi$ ,  $\phi_2 = 0$ ,  $\text{Re}(a) > 0$  (left panel);  $\gamma_1 = \pi/2$ ,  $\gamma_2 = 3\pi/8$ ,  $\phi_1 = 0$ ,  $\phi_2 = 0$ ,  $\text{Re}(a) < 0$  (right panel).

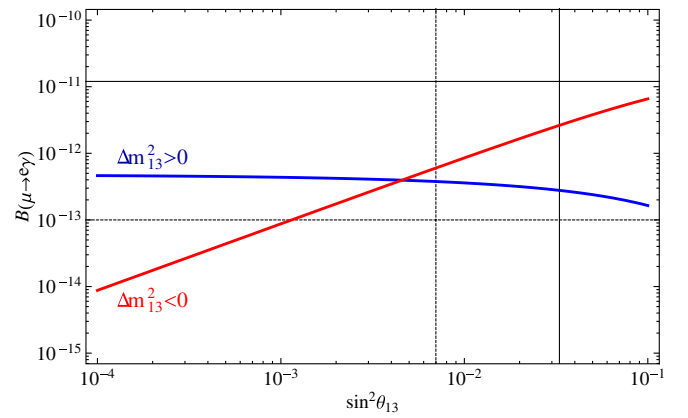


FIG. 4 (color online). The branching ratio  $B(\mu \rightarrow e\gamma)$  as a function of  $\sin^2\theta_{13}$ , in R $\tau$ L scenarios with a normal (blue) and inverted (red) light-neutrino mass spectra. The model parameters for these two cases are as in Figs. 2 (left panel) and 3 (left panel), respectively, with  $\kappa_1 = 10^{-5}$  and  $\kappa_2 = 10^{-4}$ . The horizontal solid (dashed) line denotes the current (expected future) limit on  $B(\mu \rightarrow e\gamma)$ . The vertical solid and dashed lines denote the  $2\sigma$  upper limit and the nominal best fit value of  $\sin^2\theta_{13}$ , the latter roughly corresponding to the expected sensitivity of future oscillation experiments.

The higher rates for the LFV  $\mu \rightarrow e$  transitions in a R $\tau$ L model with an inverted hierarchical light-neutrino mass spectrum may be attributed to the fact that the squared parameter  $a^2$  is proportional to the not yet well determined neutrino-mixing angle  $\sin^2\theta_{13}$ . In detail, the branching ratio  $B(\mu \rightarrow e\gamma)$  is enhanced in the case of an inverted hierarchical light-neutrino mass spectrum ( $\Delta m_{13}^2 < 0$ ). Instead, in the normal hierarchical light-neutrino scenario with  $\Delta m_{13}^2 > 0$ ,  $B(\mu \rightarrow e\gamma)$  is essentially independent of  $\sin\theta_{13}$ . This is demonstrated in Fig. 4, showing  $B(\mu \rightarrow e\gamma)$  as a function of  $\sin^2\theta_{13}$ , where  $\kappa_1 = 10^{-5}$  and  $\kappa_2 = 10^{-4}$ . In the same figure, the vertical solid and dashed lines denote the current best fit value and the expected sensitivity of future experiments for measuring  $\sin^2\theta_{13}$ , respectively. The branching ratio  $B(\mu \rightarrow e\gamma)$  depends linearly on  $\sin^2\theta_{13}$  in the inverted hierarchical light-neutrino scenario where  $\Delta m_{13}^2 < 0$ . Unlike in the normal light-neutrino scenario, the predicted value for  $\eta_B$  in the R $\tau$ L model with an inverted hierarchical light-neutrino mass spectrum falls short of explaining the BAU by 2 orders of magnitude, for a potentially observable branching ratio of  $B(\mu \rightarrow e\gamma) \sim 10^{-13}$ .

In Fig. 5 we illustrate the importance of including the full three-heavy-neutrino mixing in the calculation of the baryon asymmetry. We present a comparison between the full calculation based on using the effective Yukawa couplings  $\bar{\mathbf{h}}_{l\alpha}^\nu$  given in (4.4) (solid line) and its two-heavy-neutrino-mixing approximation (dashed line) where we set  $R_{\alpha\beta} = 0$ . Note that the two-heavy-neutrino-mixing approximation can differ from the full calculation by up to

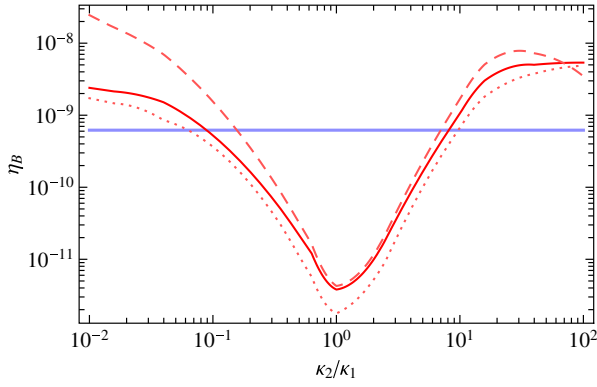


FIG. 5 (color online). The baryon asymmetry  $\eta_B$  as a function of the ratio  $\kappa_1/\kappa_2$  in a  $R\tau L$  scenario, where  $\kappa_1\kappa_2 = 10^{-8}$  is fixed. All other parameters are as in Fig. 2 (left panel). The solid line corresponds to the full numerical solution of  $\eta_B$  using the three-heavy-neutrino-mixing formula given in (4.4), the dashed line describes the two-heavy-neutrino-mixing approximation with  $R_{\alpha\beta} = 0$ , and the dotted line is obtained by neglecting the RIS-subtracted collision terms in the BE (4.27), or equivalently by setting the parameter  $\kappa\tau$  defined in (4.36) equal to 1 in the BE (4.33).

1 order of magnitude. In addition, Fig. 5 shows the baryon asymmetry  $\eta_B$  calculated by omitting the RIS-subtracted collision terms in the BE (4.27) (dotted line), or equivalently by taking the parameter  $\kappa\tau$  defined in (4.36) equal to 1 in the BE (4.33). Such a simplification may reduce the predicted values for  $\eta_B$  by as much as 60%.

Figs. 6 and 7 present numerical estimates, for a  $R\mu L$  scenario with normal and inverted light-neutrino mass spectra, respectively. We see that the baryon asymmetry  $\eta_B$  exhibits a similar dependence on  $\kappa_1$  and  $\kappa_2$  as in the  $R\tau L$  scenario. Because of the large  $e$ - and  $\tau$ -Yukawa couplings present in the  $R\mu L$  model, the largest LFV rate can be observed in the  $\tau \rightarrow e\gamma$  transitions, e.g. in the LFV process  $\tau \rightarrow e\gamma$ , with  $B(\tau \rightarrow e\gamma) \sim 10^{-10}$ . Since the current experimental sensitivity to this process is  $B_{\text{exp}}(\tau \rightarrow e\gamma) \approx 10^{-7}$  which is not expected to increase by more than 1 order of magnitude in the foreseeable future, it would be difficult to probe the parameter space of the  $R\mu L$  scenario compatible with observable BAU. On the other hand, the  $\mu \rightarrow e$  transitions in the  $R\mu L$  model, although being proportional to  $\max(\kappa_1, \kappa_2)^2 a^2$  and so smaller than the predictions obtained in  $R\tau L$  scenario, are still sizeable enough to produce a  $\mu \rightarrow e$  conversion rate of  $B_{\mu e}({}^{48}\text{Ti}) \approx 2 \times 10^{-17}$  (for  $\Delta m_{13}^2 > 0$ ) and  $5 \times 10^{-16}$  (for  $\Delta m_{13}^2 < 0$ ). As the parameters  $a$  and  $b$  are approximately inversely proportional to  $\kappa_{1,2}$ , these values are largely independent of  $\kappa_{1,2}$  and apply to the whole  $(\kappa_1, \kappa_2)$  parameter plane, as depicted in Figs. 6 and 7. Consequently, this scenario could be probed at a future  $\mu \rightarrow e$  conversion experiment with a sensitivity of  $\sim 10^{-16}$  (COMET, mu2e), or  $\sim 10^{-18}$  (PRISM) [21].

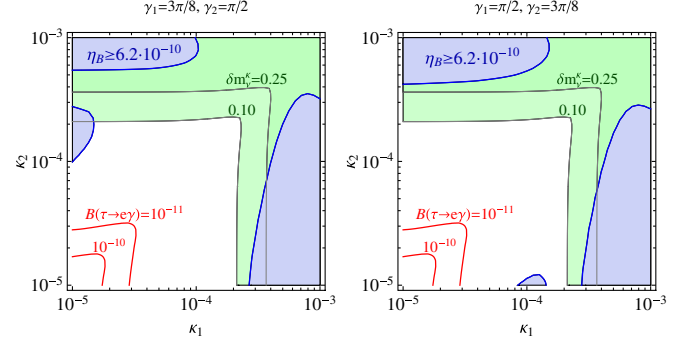


FIG. 6 (color online). The baryon asymmetry  $\eta_B$  and the branching ratio  $B(\tau \rightarrow e\gamma)$  as functions of  $\kappa_1$  and  $\kappa_2$  in the  $R\mu L$  model with  $m_N = 120$  GeV, where a normal light-neutrino mass spectrum is assumed. The remaining parameters were chosen as follows:  $\gamma_1 = 3\pi/8$ ,  $\gamma_2 = \pi/2$ ,  $\phi_1 = \pi$ ,  $\phi_2 = 0$ ,  $\text{Re}(a) > 0$  (left panel);  $\gamma_1 = \pi/2$ ,  $\gamma_2 = 3\pi/8$ ,  $\phi_1 = 0$ ,  $\phi_2 = 0$ ,  $\text{Re}(a) < 0$  (right panel). The neutrino oscillation parameters are set at their best fit values, with  $\sin^2\theta_{13} = 0.033$  at its  $2\sigma$  upper limit. The dark (blue) shaded regions denote the parameter space where the baryon asymmetry is larger than the observational value  $\eta_B = 6.2 \times 10^{-10}$ . The light (green) shaded areas labeled as ‘ $\delta m_\nu^\kappa = 0.25$ ’ and ‘0.10’ indicate the parameter space where the inversion of the light-neutrino mass matrix is violated at the 25% and 10% levels, respectively.

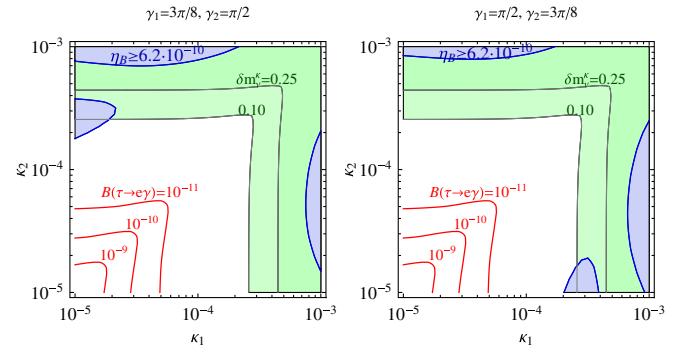


FIG. 7 (color online). The same as in Fig. 6, but for an inverted light-neutrino mass spectrum and the following choice of parameters:  $\gamma_1 = 3\pi/8$ ,  $\gamma_2 = \pi/2$ ,  $\phi_1 = \pi$ ,  $\phi_2 = 0$ ,  $\text{Re}(a) > 0$  (left panel);  $\gamma_1 = \pi/2$ ,  $\gamma_2 = 3\pi/8$ ,  $\phi_1 = 0$ ,  $\phi_2 = 0$ ,  $\text{Re}(a) < 0$  (right panel).

Finally, Figs. 8 and 9 display numerical estimates, for a  $ReL$  scenario with normal and inverted light-neutrino mass spectra, respectively. Our results are quite analogous to the  $R\mu L$  case. Correspondingly, the largest LFV rate is obtained for the process  $\tau \rightarrow \mu\gamma$ . However, successful  $ReL$  requires  $B(\tau \rightarrow \mu\gamma) \sim 10^{-14}$ , which is far beyond the reach of the next generation experiments. In analogy to the  $R\mu L$  case, the rates for coherent  $\mu \rightarrow e$  conversion in nuclei are found to be sizeable. Specifically, we obtain  $B_{\mu e}({}^{48}\text{Ti}) \approx 3 \times 10^{-17}$  (for  $\Delta m_{13}^2 > 0$ ) and  $7 \times 10^{-16}$

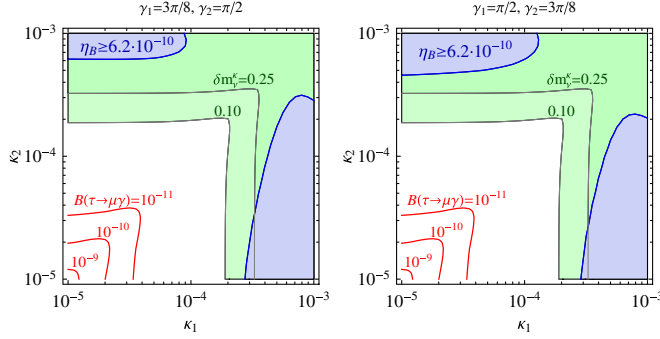


FIG. 8 (color online). The baryon asymmetry  $\eta_B$  and the branching ratio  $B(\tau \rightarrow \mu\gamma)$  as functions of  $\kappa_1$  and  $\kappa_2$  in the  $R\ell L$  model with  $m_N = 120$  GeV, considering a normal light-neutrino mass spectrum. The remaining parameters were chosen as follows:  $\gamma_1 = 3\pi/8$ ,  $\gamma_2 = \pi/2$ ,  $\phi_1 = \pi$ ,  $\phi_2 = 0$ ,  $\text{Re}(a) > 0$  (left panel);  $\gamma_1 = \pi/2$ ,  $\gamma_2 = 3\pi/8$ ,  $\phi_1 = 0$ ,  $\phi_2 = 0$ ,  $\text{Re}(a) < 0$  (right panel). The neutrino oscillation parameters are chosen at their best fit values but with  $\sin^2\theta_{13} = 0.033$  at its  $2\sigma$  upper limit. The dark (blue) shaded regions denote the parameter space where the baryon asymmetry is larger than  $\eta_B^{\text{obs}} = 6.2 \times 10^{-10}$ . The light (green) shaded areas labeled as ‘ $\delta m_\nu^2 = 0.25$ ’ and ‘0.10’ indicate the parameter space where the inversion of the light-neutrino mass matrix is violated at the 25% and 10% levels, respectively.

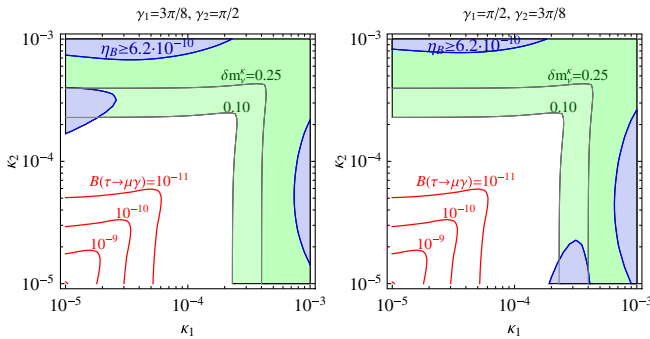


FIG. 9 (color online). The same as in Fig. 8, but for an inverted light-neutrino mass spectrum and the following choice of parameters:  $\gamma_1 = 3\pi/8$ ,  $\gamma_2 = \pi/2$ ,  $\phi_1 = \pi$ ,  $\phi_2 = 0$ ,  $\text{Re}(a) > 0$  (left panel);  $\gamma_1 = \pi/2$ ,  $\gamma_2 = 3\pi/8$ ,  $\phi_1 = 0$ ,  $\phi_2 = 0$ ,  $\text{Re}(a) < 0$  (right panel).

(for  $\Delta m_{13}^2 < 0$ ). Interestingly enough, these rates are well within reach of the proposed PRISM experiment [21].

## VI. CONCLUSIONS

We have analyzed minimal low-scale seesaw scenarios of resonant leptogenesis and studied their potential implications for observables of charged LFV, such as  $\mu \rightarrow e\gamma$  and  $\mu \rightarrow e$  conversion in nuclei. We have considered three physically interesting flavor realizations of resonant leptogenesis, where the observed BAU originates from an

individual  $\tau$ -,  $\mu$ - or  $e$ -lepton-number asymmetry which gets resonantly enhanced via the out-of-equilibrium decays of nearly degenerate heavy Majorana neutrinos.

By means of approximate lepton-flavor symmetries, we have been able to construct viable and natural models of  $R\ell L$  compatible with universal right-handed neutrino masses at the GUT scale, where the required heavy-neutrino mass splittings are generated via RG effects. Particular attention has been paid that the effective resummation method introduced in [7] and used in our study to compute the resonantly enhanced lepton asymmetries respects the Nanopoulos-Weinberg no-go theorem [54] in the  $L$ -conserving limit of the theory. Specifically, we have checked that the leptonic asymmetries  $\delta_{\alpha l}$  given in (4.8) and (4.9) vanish in all parametrically possible  $L$ -conserving limits of the  $R\ell L$  scenarios. In agreement with earlier studies [13,14], we find that at least three heavy Majorana neutrinos are required, in order to potentially have both successful leptogenesis and experimentally testable rates for LFV processes, such as  $\mu \rightarrow e\gamma$  and  $\mu \rightarrow e$  conversion in nuclei.

We have found that the heavy Majorana neutrinos in  $R\ell L$  scenarios can be as light as 100 GeV, while their couplings to two of the charged leptons may be large so as to lead to LFV effects that could be tested by the MEG and the COMET/PRISM experiments. Specifically, in the  $R\tau L$  model with a normal light-neutrino mass hierarchy, there is a sizeable model parameter space with successful leptogenesis and large LFV process rates, with  $B(\mu \rightarrow e\gamma) \approx 10^{-12}$ . This prediction is largely independent of  $\sin^2\theta_{13}$  and the other light-neutrino oscillation parameters. On the other hand, in the  $R\tau L$  model with inversely hierarchical light neutrinos,  $B(\mu \rightarrow e\gamma)$  is linearly proportional to  $\sin^2\theta_{13}$ , and can be enhanced by more than 1 order of magnitude compared to the normal hierarchy case for  $\sin^2\theta_{13}$  close to its upper experimental  $2\sigma$  limit. Unfortunately, the generated baryon asymmetry  $\eta_B$  is suppressed in this scenario, and to test the viable parameter space for successful leptogenesis would require an experiment for  $\mu \rightarrow e$  conversion in nuclei which is sensitive to  $B_{\mu e} \approx 10^{-17} - 10^{-16}$ . This feature is also quite generic for the case of the  $R\mu L$  and  $R\ell L$  models, where  $\mu \rightarrow e$  flavor transitions are suppressed by the small  $\tau$ -Yukawa couplings  $\kappa_{1,2}$ . In all  $R\ell L$  models, charged LFV in the  $\tau$ -lepton sector turns out to be at least 6 orders of magnitude beyond the current experimental sensitivity, as the predicted branching ratios are  $B(\tau \rightarrow e\gamma, \mu\gamma) \lesssim 10^{-14}$  in parameter regions required for successful leptogenesis.

Further studies will be needed to analyze the full range of theoretical, phenomenological and cosmological implications of the three different universal models of  $R\ell L$ ,  $R\mu L$  and  $R\tau L$ . For instance, the consideration of thermal effects [58] may provide a significant improvement on the standard framework of classical BEs adopted in the present analysis. An equally significant issue is whether



our minimal RL models can account for the well-known problem of cold dark matter in the Universe. An obvious solution would be to consider supersymmetric versions of R $\ell$ L scenarios [59,60] and study the relic abundance of the lightest stable supersymmetry particle, which could be a thermal right-handed sneutrino [61]. Alternatively, one may consider scale-invariant extensions of the SM with right-handed neutrinos [62,63], which are minimally augmented with one complex singlet scalar field whose one-loop induced vacuum expectation value can naturally explain the origin of the electroweak-scale mass of the heavy Majorana neutrinos. It has been shown recently [63] that a minimal  $\mathbf{Z}_4$ -symmetric variant of these models can stay

perturbative up to the Planck scale, as well as provide a cold dark matter candidate through the so-called Higgs-portal mechanism [64]. It is therefore rather motivating to perform a dedicated analysis of observing electroweak-scale heavy Majorana neutrinos within the specific context of the R $\ell$ L scenarios studied here, through their possible like-sign dilepton [26,65] and/or trilepton [66] signatures at the LHC or at other future high-energy colliders.

## ACKNOWLEDGMENTS

This work is supported in part by the STFC research Grant No. PP/D000157/1.

- 
- [1] G. Hinshaw *et al.* (WMAP Collaboration), *Astrophys. J. Suppl. Ser.* **180**, 225 (2009).
- [2] E. Komatsu *et al.*, *Astrophys. J. Suppl. Ser.* **192**, 18 (2011).
- [3] For reviews, see, W. Buchmuller, R. D. Peccei, and T. Yanagida, *Annu. Rev. Nucl. Part. Sci.* **55**, 311 (2005); T. Ibrahim and P. Nath, *Rev. Mod. Phys.* **80**, 577 (2008); R. Allahverdi, R. Brandenberger, F. Y. Cyr-Racine, and A. Mazumdar, *Annu. Rev. Nucl. Part. Sci.* **60**, 27 (2010).
- [4] M. Fukugita and T. Yanagida, *Phys. Lett. B* **174**, 45 (1986).
- [5] P. Minkowski, *Phys. Lett. B* **67**, 421 (1977); M. Gell-Mann, P. Ramond, and R. Slansky, in *Supergravity*, edited by D. Z. Freedman and P. van Nieuwenhuizen (North-Holland, Amsterdam, 1979); T. Yanagida, in *Proceedings of the Workshop on the Unified Theory and the Baryon Number in the Universe*, edited by O. Sawada and A. Sugamoto (KEK, Tsukuba, Japan, 1979); R. N. Mohapatra and G. Senjanović, *Phys. Rev. Lett.* **44**, 912 (1980).
- [6] V. A. Kuzmin, V. A. Rubakov, and M. E. Shaposhnikov, *Phys. Lett. B* **155**, 36 (1985).
- [7] A. Pilaftsis, *Phys. Rev. D* **56**, 5431 (1997).
- [8] A. Pilaftsis and T. E. J. Underwood, *Nucl. Phys.* **B692**, 303 (2004).
- [9] J. Liu and G. Segré, *Phys. Rev. D* **48**, 4609 (1993).
- [10] M. Flanz, E. A. Paschos, and U. Sarkar, *Phys. Lett. B* **345**, 248 (1995); L. Covi, E. Roulet, and F. Vissani, *Phys. Lett. B* **384**, 169 (1996).
- [11] A. Pilaftsis, *Int. J. Mod. Phys. A* **14**, 1811 (1999).
- [12] M. Y. Khlopov and A. D. Linde, *Phys. Lett. B* **138**, 265 (1984); J. R. Ellis, J. E. Kim, and D. V. Nanopoulos, *Phys. Lett. B* **145**, 181 (1984); J. R. Ellis, D. V. Nanopoulos, and S. Sarkar, *Nucl. Phys.* **B259**, 175 (1985).
- [13] A. Pilaftsis, *Phys. Rev. Lett.* **95**, 081602 (2005).
- [14] A. Pilaftsis and T. E. J. Underwood, *Phys. Rev. D* **72**, 113001 (2005).
- [15] S. Y. Khlebnikov and M. E. Shaposhnikov, *Nucl. Phys.* **B308**, 885 (1988).
- [16] J. A. Harvey and M. S. Turner, *Phys. Rev. D* **42**, 3344 (1990).
- [17] H. Dreiner and G. G. Ross, *Nucl. Phys.* **B410**, 188 (1993).
- [18] M. Laine and M. E. Shaposhnikov, *Phys. Rev. D* **61**, 117302 (2000).
- [19] C. Aalseth *et al.*, arXiv:hep-ph/0412300.
- [20] See proposal by MEG collaboration at <http://meg.web.psi.ch/docs/index.html>.
- [21] Y. Kuno, *Nucl. Phys. B, Proc. Suppl.* **149**, 376 (2005).
- [22] R. Gonzalez Felipe, F. R. Joaquim, and B. M. Nobre, *Phys. Rev. D* **70**, 085009 (2004); K. Turzyski, *Phys. Lett. B* **589**, 135 (2004); G. C. Branco, R. Gonzalez Felipe, F. R. Joaquim, and B. M. Nobre, *Phys. Lett. B* **633**, 336 (2006); G. C. Branco, A. J. Buras, S. Jager, S. Uhlig, and A. Weiler, *J. High Energy Phys.* **09** (2007) 004.
- [23] R. Barbieri, P. Creminelli, A. Strumia, and N. Tetradis, *Nucl. Phys.* **B575**, 61 (2000); E. Nardi, Y. Nir, J. Racker, and E. Roulet, *J. High Energy Phys.* **01** (2006) 068; A. Abada, S. Davidson, F. X. Josse-Michaux, M. Losada, and A. Riotto, *J. Cosmol. Astropart. Phys.* **04** (2006) 004.
- [24] T. Endoh, T. Morozumi, and Z. h. Xiong, *Prog. Theor. Phys.* **111**, 123 (2004); O. Vives, *Phys. Rev. D* **73**, 073006 (2006).
- [25] P. H. Chankowski and Z. Pluciennik, *Phys. Lett. B* **316**, 312 (1993); K. S. Babu, C. N. Leung, and J. T. Pantaleone, *Phys. Lett. B* **319**, 191 (1993); S. Antusch, M. Drees, J. Kersten, M. Lindner, and M. Ratz, *Phys. Lett. B* **519**, 238 (2001); S. Antusch, J. Kersten, M. Lindner, M. Ratz, and M. A. Schmidt, *J. High Energy Phys.* **03** (2005) 024.
- [26] A. Pilaftsis, *Z. Phys. C* **55**, 275 (1992).
- [27] For a recent analysis, see, M. Maltoni, T. Schwetz, M. A. Tortola, and J. W. Valle, *New J. Phys.* **6**, 122 (2004).
- [28] M. C. Gonzalez-Garcia, M. Maltoni, and J. Salvado, *J. High Energy Phys.* **04** (2010) 056.
- [29] M. Doi, T. Kotani, and E. Takasugi, *Prog. Theor. Phys. Suppl.* **83**, 1 (1985).
- [30] For example, see the textbook by K. Grotz and H. V. Klapdor, *The Weak Interaction in Nuclear, Particle and Astrophysics* (Adam Hilger, Bristol, 1989).
- [31] H. V. Klapdor-Kleingrothaus, *Sixty Years of Double Beta Decay* (World Scientific, Singapore, 2001); H. V. Klapdor-Kleingrothaus, A. Dietz, H. L. Harney, and I. V.

- Krivosheina, *Mod. Phys. Lett. A* **16**, 2409 (2001); H. V. Klapdor-Kleingrothaus, A. Dietz, and I. Krivosheina, *Part. Nucl. Lett.* **110**, 57 (2002); *Found. Phys.* **32**, 1181 (2002).
- [32] B. Pontecorvo, *Sov. Phys. JETP* **7**, 172 (1958); Z. Maki, M. Nakagawa, and S. Sakata, *Prog. Theor. Phys.* **28**, 870 (1962).
- [33] H. V. Klapdor-Kleingrothaus, A. Dietz, I. V. Krivosheina, and O. Chkvorets, *Nucl. Instrum. Methods Phys. Res., Sect. A* **522**, 371 (2004).
- [34] T. P. Cheng and L. F. Li, *Phys. Rev. Lett.* **45**, 1908 (1980).
- [35] A. Ilakovac and A. Pilaftsis, *Nucl. Phys.* **B437**, 491 (1995).
- [36] K. Nakamura *et al.* (Particle Data Group), *J. Phys. G* **37**, 075021 (2010).
- [37] G. Feinberg and S. Weinberg, *Phys. Rev. Lett.* **3**, 111 (1959); **3**, 527 (1959); W. J. Marciano and A. I. Sanda, *Phys. Rev. Lett.* **38**, 1512 (1977); O. Shanker, *Phys. Rev. D* **20**, 1608 (1979); J. Bernabéu, E. Nardi, and D. Tommasini, *Nucl. Phys.* **B409**, 69 (1993).
- [38] For reviews, see, J. D. Vergados, *Phys. Rep.* **133**, 1 (1986); T. S. Kosmas, G. K. Leontaris, and J. D. Vergados, *Prog. Part. Nucl. Phys.* **33**, 397 (1994).
- [39] A. Ilakovac and A. Pilaftsis, *Phys. Rev. D* **80**, 091902 (2009).
- [40] J. C. Sens, *Phys. Rev.* **113**, 679 (1959); K. W. Ford and J. G. Wills, *Nucl. Phys.* **35**, 295 (1962); J. Bernabéu, *Il Nuovo cimento, A* **4**, 715 (1971); H. C. Chiang, E. Oset, T. S. Kosmas, A. Faessler, and J. D. Vergados, *Nucl. Phys.* **A559**, 526 (1993).
- [41] T. Suzuki, D. F. Measday, and J. P. Roalsvig, *Phys. Rev. C* **35**, 2212 (1987).
- [42] For instance, see, B. Frois and C. N. Papanicolas, *Annu. Rev. Nucl. Part. Sci.* **37**, 133 (1987), and references therein.
- [43] C. Dohmen *et al.* (SINDRUM II Collaboration), *Phys. Lett. B* **317**, 631 (1993).
- [44] A. Kurup, in *Proceedings of 1st International Particle Accelerator Conference: IPAC'10, Kyoto, Japan, 23-28 May 2010*, (IPAC'10 OC/ACFA, Kyoto, 2010) p. WEPE055 <http://accelconf.web.cern.ch/AccelConf/IPAC10/papers/wepe055.pdf>.
- [45] D. Glenzinski, *AIP Conf. Proc.* **1222**, 383 (2010).
- [46] A. Pilaftsis, *Phys. Rev. D* **78**, 013008 (2008).
- [47] A. Pilaftsis, *Nucl. Phys.* **B504**, 61 (1997).
- [48] M. Flanz, E. A. Paschos, U. Sarkar, and J. Weiss, *Phys. Lett. B* **389**, 693 (1996).
- [49] W. Buchmüller and M. Plümacher, *Phys. Lett. B* **431**, 354 (1998).
- [50] A. Anisimov, A. Broncano, and M. Plümacher, *Nucl. Phys.* **B737**, 176 (2006).
- [51] S. Blanchet, T. Hambye, and F. X. Josse-Michaux, *J. High Energy Phys.* **04** (2010) 023.
- [52] S. Blanchet, P. S. B. Dev, and R. N. Mohapatra, *Phys. Rev. D* **82**, 115025 (2010).
- [53] R. N. Mohapatra and J. W. F. Valle, *Phys. Rev. D* **34**, 1642 (1986); S. Nandi and U. Sarkar, *Phys. Rev. Lett.* **56**, 564 (1986).
- [54] D. V. Nanopoulos and S. Weinberg, *Phys. Rev. D* **20**, 2484 (1979).
- [55] *Handbook of Mathematical Functions*, edited by M. Abramowitz and I. A. Stegun (Verlag Harri Deutsch, Frankfurt, 1984).
- [56] F. F. Deppisch, Diplom thesis, University of Würzburg, 2000, available from <http://theorie.physik.uni-wuerzburg.de/wehner/publications/Dipl/deppisch.ps.gz>.
- [57] E. W. Kolb and S. Wolfram, *Nucl. Phys.* **B172**, 224 (1980);
- [58] G. F. Giudice, A. Notari, M. Raidal, A. Riotto, and A. Strumia, *Nucl. Phys.* **B685**, 89 (2004); V. Cirigliano, A. De Simone, G. Isidori, I. Masina, and A. Riotto, *J. Cosmol. Astropart. Phys.* **01** (2008) 004; M. Garny, A. Hohenegger, A. Kartavtsev, and M. Lindner, *Phys. Rev. D* **81**, 085027 (2010); M. Beneke, B. Garbrecht, M. Herranen, and P. Schwaller, *Nucl. Phys.* **B838**, 1 (2010).
- [59] B. Garbrecht, C. Pallis, and A. Pilaftsis, *J. High Energy Phys.* **12** (2006) 038.
- [60] J. R. Ellis, M. Raidal, and T. Yanagida, *Phys. Lett. B* **546**, 228 (2002); Y. Grossman, T. Kashti, Y. Nir, and E. Roulet, *Phys. Rev. Lett.* **91**, 251801 (2003); G. D'Ambrosio, G. F. Giudice, and M. Raidal, *Phys. Lett. B* **575**, 75 (2003); T. Hambye, J. March-Russell, and S. M. West, *J. High Energy Phys.* **07** (2004) 070; E. J. Chun, *Phys. Rev. D* **69**, 117303 (2004); K. S. Babu, A. G. Bachri, and Z. Tavartkiladze, *Int. J. Mod. Phys. A* **23**, 1679 (2008); C. S. Fong and M. C. Gonzalez-Garcia, *J. High Energy Phys.* **06** (2008) 076; C. S. Fong, M. C. Gonzalez-Garcia, E. Nardi, and J. Racker, *J. Cosmol. Astropart. Phys.* **12** (2010) 013.
- [61] F. F. Deppisch and A. Pilaftsis, *J. High Energy Phys.* **10** (2008) 080; D. G. Cerdeno, C. Munoz, and O. Seto, *Phys. Rev. D* **79**, 023510 (2009).
- [62] R. Foot, A. Kobakhidze, K. L. McDonald, and R. R. Volkas, *Phys. Rev. D* **76**, 075014 (2007); K. A. Meissner and H. Nicolai, *Eur. Phys. J. C* **57**, 493 (2008).
- [63] L. Alexander-Nunneley and A. Pilaftsis, *J. High Energy Phys.* **09** (2010) 021.
- [64] V. Silveira and A. Zee, *Phys. Lett. B* **161**, 136 (1985); J. McDonald, *Phys. Rev. D* **50**, 3637 (1994).
- [65] A. Datta, M. Guchait, and A. Pilaftsis, *Phys. Rev. D* **50**, 3195 (1994); F. del Aguila, J. A. Aguilar-Saavedra, and R. Pittau, *J. High Energy Phys.* **10** (2007) 047; S. Bray, J. S. Lee, and A. Pilaftsis, *Nucl. Phys.* **B786**, 95 (2007); J. Kersten and A. Y. Smirnov, *Phys. Rev. D* **76**, 073005 (2007); A. Atre, T. Han, S. Pascoli, and B. Zhang, *J. High Energy Phys.* **05** (2009) 030.
- [66] F. del Aguila and J. A. Aguilar-Saavedra, *Nucl. Phys.* **B813**, 22 (2009).